isvr Institute of Sound and Vibration Research

Structural Analysis of a Four-Beam and Plate Coupled Structure using a Modal Method and an Approximate Wave Method

J.W. Yoo, D.J. Thompson and N.S. Ferguson

ISVR Technical Memorandum No 944

December 2004

University of Southampton

SCIENTIFIC PUBLICATIONS BY THE ISVR

Technical Reports are published to promote timely dissemination of research results by ISVR personnel. This medium permits more detailed presentation than is usually acceptable for scientific journals. Responsibility for both the content and any opinions expressed rests entirely with the author(s).

Technical Memoranda are produced to enable the early or preliminary release of information by ISVR personnel where such release is deemed to the appropriate. Information contained in these memoranda may be incomplete, or form part of a continuing programme; this should be borne in mind when using or quoting from these documents.

Contract Reports are produced to record the results of scientific work carried out for sponsors, under contract. The ISVR treats these reports as confidential to sponsors and does not make them available for general circulation. Individual sponsors may, however, authorize subsequent release of the material.

UNIVERSITY OF SOUTHAMPTON

INSTITUTE OF SOUND AND VIBRATION RESEARCH

DYNAMICS GROUP

Structural Analysis of a Four-Beam and Plate Coupled Structure using a Modal Method and an Approximate Wave Method

by

J.W. Yoo, D.J. Thompson and N.S. Ferguson

ISVR Technical Memorandum No: 944

December 2004

Authorised for issue by
Professor M.J. Brennan
Group Chairman

CONTENTS

1. INTRODUCTION

Several numerical methods have been used to investigate the structural behaviour of a coupled structure consisting of beams and a plate. A wave technique was introduced for a structure consisting of one or two parallel beams attached to the edges of a rectangular plate [1, 2]. A Fourier approach was applied for the two-beam structure, including the case where two dissimilar beams are attached to a rectangular plate [3].

A fully framed structure consisting of four beams surrounding a rectangular plate is an important concern in the present research, as it is a principal configuration considered in many engineering structures, e.g. automotive vehicles, ship hulls, etc. Although the numerical approaches mentioned above produced good results for the vibrational motion in the cases considered, they have rarely been used for the analysis of framed structures consisting of four beams.

Previous reports [1, 2] show that the wave approach can be used to obtain an approximate response of a beam-plate coupled structure as long as the system consists of a subsystem (spine) possessing long wavelength waves and the receiver subsystem possessing short wavelength waves. Thus, in principle, this technique can be applied to give an approximate dynamic response for a fully framed structure. It is necessary to have an accurate result for comparison with this approximate wave-based solution. Thus, in the present report a modal method is developed using a Lagrangian formulation. Initially, mode shape functions of a beam and a plate are obtained considering appropriate boundary conditions. Then, analytical equations are developed to find the vibrational response of a coupled structure consisting of four beams and a rectangular plate. This is also an approximate technique, given that in practice the infinite modal summation is not practical and a finite sum of modes is used. Nevertheless one can perform numerical checks to inspect convergence and limit any errors to be insignificant.

There are some published studies on a framed structure consisting of four beams and a plate. Takabatake and Nagareda studied the framed structure, where the behaviour of the plate was the primary focus [4]. The plate supported with edge beams was replaced by a plate with edges elastically restrained against translation and rotation. Using relationships between these different boundary conditions, the shape functions in the plate use the beam shape functions corresponding to supports with equivalent translational and torsional stiffness. The closed form approximate solutions for static and dynamic problems of a rectangular plate with edge

beams were developed using the Galerkin method, in which the mass effect of the beam is neglected.

The static and dynamic characteristics of a rectangular plate with edge beams were evaluated using a Ritz vector approach by Yang and Gupta [5]. The effect of elastic edge restraints is accounted for by including appropriate integrals for the beams in the expressions for the total kinetic and potential energies, although the procedure to develop the modal mass and modal stiffness is not clearly explained. The various types of boundary conditions at the beams are considered by the corresponding Ritz vectors. The contribution of beam mass to the total kinetic energy is also considered.

Both studies [4, 5] concentrated on predicting the plate behaviour, rather than that of the beam. Also, both papers assumed that the motion of the ends of each beam is zero. From the point of view that the stiff beams possessing the bending waves radiate short-wavelength bending waves into the plate, the behaviour of the beams is very important [6]. Therefore, the present study, which considers the beam as well as the plate and allows for excitation at the beam ends, differs from the studies described above.

The wave approach for the investigation of the structure consisting of a so-called spine and receiver was initially introduced by Grice and Pinnington [7]. The coupled system considered was a box structure and the finite element method was used to predict a long-wave response and analytical impedances were considered to calculate short flexural waves. This concept is considered in the present report. However, here the coupled wavenumber representing the long wavelength wave including the effect of the plate impedance is obtained to describe the motion instead of using the finite element model.

The present report is divided into two main parts. Firstly the description of a modal approach is given. The mode shape functions of a beam and a plate are introduced in sections 2 and 3, and the Lagrangian formulation is applied to obtain the equation of motion of the system. Then, a coupling procedure is followed in section 4. How many modes should be included in the calculation is an important issue in the mode-based analysis. Numerical results are shown and compared with those based on the Fourier technique previously investigated [3], although the structure consisting of only two beams is used as there is no result previously obtained for the four-beam structure. Then, the dynamic response of the four-beam structure using the modal method is compared with that of the finite element method (FEM).

In the second part, the procedure for obtaining an approximate response using the wave technique is explained in section 5. The principal equations, such as the equation of motion of a beam and the expression for the plate impedance, are briefly given and numerical

results are shown for comparison of the various techniques. The corresponding equations of motion, based on the wave method for the framed structure, are represented in Appendix B.

Depending upon the problem and application, the detailed response at individual frequencies is important at low frequencies. However, with increasing frequency the band-averaged response and the variability about a mean value are much more important than narrow band results. An aim of the present study is related to the dynamic characteristic in the mid and high frequency regions. Thus, results based on the wave method are mostly represented from this point of view. For example, a result such as an octave band average or a confidence interval of a response are just as applicable and useful. Hence these results are also presented in the report.

The methods in sections 4 and 5 are applied to a perspex plate 1.0×0.75 m with a thickness of 2 mm, surrounded by beams 22×6 mm. The frequency range selected is 5.6 to 1412 Hz (1/3 octave bands 6.3 to 1250 Hz). In this range each beam has between 7 and 9 modes so that the beams can be considered to be in their "low frequency" range. The plate has a modal density of about 0.4 modes per Hz, so that its 10^{th} mode occurs by about 23 Hz and about 500 modes can be expected below 1412 Hz. This, therefore, has "high frequency" behaviour from the middle of the frequency range considered.

2. A MODAL DESCRIPTION FOR BEAM VIBRATION

2.1 Mode shape function and natural frequencies

It is well known [8] that the dynamic response of an elastic structure, such as a beam, at position x and time t can be expressed as

$$w(x,t) = \sum_m \phi_m(x) q_m(t) \tag{2.1}$$

where $w(x,t)$ is the displacement, $q_m(t)$ is the generalised coordinate for mode m and $\phi_m(x)$ the corresponding mode shape function of the structure for given specified boundary conditions. The modal expansion given in equation (2.1) is valid for arbitrary motion as well as harmonic steady state motion in particular. Strictly the summation is over the infinite number of modes of the structure.

The general expression for the normal mode or characteristic function of a uniform beam is given by [8]

$$\phi(x) = C_1 \cos k_x x + C_2 \sin k_x x + C_3 \cosh k_x x + C_4 \sinh k_x x\,. \tag{2.2}$$

where k_x is the flexural wavenumber related to the natural frequencies by

$$\omega_m^2 = k_x^4 \frac{D_b}{m_b'}. \tag{2.3}$$

where D_b is the bending stiffness, ω_m is the m th natural frequency and m_b' is the mass per unit length of the beam assuming a uniform cross-sectional area. Using the general solution, such as equation (2.2), the mode shape functions for arbitrary boundary conditions can be found [8]. Solving the resulting characteristic equation provides the values of k_x for the particular modes.

In the present report, both ends of the beam, taken as $x = 0$ and $x = L_x$, are considered to be in sliding conditions and the corresponding boundary conditions are

$$\left.\frac{d\phi}{dx}\right|_{x=0} = 0, \tag{2.4a}$$

$$\left.\frac{d^3\phi}{dx^3}\right|_{x=0} = 0, \tag{2.4b}$$

$$\left.\frac{d\phi}{dx}\right|_{x=L_x} = 0, \tag{2.4c}$$

$$\left.\frac{d^3\phi}{dx^3}\right|_{x=L_x} = 0. \tag{2.4d}$$

where L_x is the length of the beam.

From equation (2.4 a)

$$\left.\frac{d\phi}{dx}\right|_{x=0} = C_2 k_x + C_4 k_x = 0,\ C_4 = -C_2. \tag{2.5}$$

From equation (2.4 b)

$$\left.\frac{d^3\phi}{dx^3}\right|_{x=0} = -C_2 k_x^3 + C_4 k_x^3 = 0,\ C_4 = C_2. \tag{2.6}$$

From equations (2.5) and (2.6), therefore

$$C_4 = C_2 = 0. \tag{2.7}$$

Substituting this into equation (2.2) and making use of boundary condition equations (2.4c) and (2.4d) results in

$$\left.\frac{d\phi}{dx}\right|_{x=L_x} = -C_1 k_x \sin k_x L_x + C_3 k_x \sinh k_x L_x = 0$$

$$-C_1 \sin k_x L_x + C_3 \sinh k_x L_x = 0. \tag{2.8}$$

and

$$\left.\frac{d^3\phi}{dx^3}\right|_{x=L_x} = C_1 k_x^3 \sin k_x L_x + C_3 k_x^3 \sinh k_x L_x = 0$$

$$C_1 \sin k_x L_x + C_3 \sinh k_x L_x = 0. \tag{2.9}$$

Adding equations (2.8) and (2.9) gives

$$C_3 \sinh k_x L_x = 0 \tag{2.10}$$

yielding

$$C_3 = 0 \tag{2.11}$$

as $\sinh k_x L_x \neq 0$ except for $k_x = 0$. The characteristic equation is therefore

$$\sin k_x L_x = 0. \tag{2.12}$$

The corresponding solutions for $k_x L_x$ are

$$k_x L_x = 0,\ \pi,\ 2\pi,\ 3\pi,\ \cdots.$$

and thus, the wavenumbers can be found as [9, 10]

$$k_x = \frac{m\pi}{L_x} \quad \text{for } m = 0,\ 1,\ 2,\ 3,\ \cdots \tag{2.13}$$

where $m = 0$ is considered as a rigid mode of a sliding beam.

The resulting mode shape from equation (2.2) is

$$\phi(x) = \cos k_x x. \tag{2.14}$$

2.2 Equation of motion using the Lagrangian formulation *

The response of the structure, given knowledge of the mode shape functions, requires the generalised coordinate $q_m(t)$ to be determined as a solution of Lagrange's equations of motion. The equations are derived by expressing the Lagrangian L in terms of the kinetic and potential energy of the structure [11].

As the time derivative of the motion can be written as

$$\frac{\partial w}{\partial t} = \sum_m \dot{q}_m \phi_m \tag{2.15}$$

the kinetic energy of the beam is given by

$$\begin{aligned} T &= \frac{1}{2}\int_0^{L_x} m_b' \left(\frac{\partial w}{\partial t}\right)^2 dx \\ &= \frac{1}{2}\int_0^{L_x} m_b' \sum_m \sum_n \phi_m \phi_n \dot{q}_m \dot{q}_n dx = \frac{1}{2}\sum_m \sum_n \dot{q}_m \dot{q}_n \int_0^{L_x} m_b' \phi_m \phi_n dx \end{aligned} \tag{2.16}$$

which is expressed in terms of the m th and n th mode shape function. As the normal modes $\phi_m(x)$ such as given in equation (2.14) are orthogonal,

* The procedure to derive the equation of motion based on the Lagrangian is explained in [8]. This is also known as the assumed-modes method.

$$\int_0^{L_x} m_b'(x)\phi_m\phi_n dx = \begin{cases} 0 & for\, n \neq m \\ M_m^b & for\, n = m \end{cases} \tag{2.17}$$

where M_m^b is the generalised or modal mass in the m th mode of the structure. For the mode shape of equation (2.14) $M_m^b = m_b' L_x/2$ for $m \geq 1$ and $m_b' L_x$ for $m = 0$.

Therefore, the kinetic energy of an elastic structure can be expressed as

$$T = \frac{1}{2}\sum_{m=0}^{\infty} M_m^b \dot{q}_m^2 \text{ for } m = 0, 1, 2, 3, \cdots \tag{2.18}$$

Similarly, the potential energy is written as

$$U = \frac{1}{2}\int_0^{L_x} D_b \left(\frac{\partial^2 w}{\partial x^2}\right)^2 dx = \frac{D_b}{2}\sum_m \sum_n q_m q_n \int_0^{L_x} \frac{d^2\phi_m}{dx^2}\frac{d^2\phi_n}{dx^2} dx \tag{2.19}$$

Due to orthogonality of the modes the potential energy can simply be written as

$$U = \frac{1}{2}\sum_{m=1}^{\infty} K_m^b q_m^2 \tag{2.20}$$

where K_m^b is the generalised stiffness of the m th mode of the structure and is defined by

$$K_m^b = D_b \int_0^{L_x} \left(\frac{d^2\phi_m}{dx^2}\right)^2 dx \text{ for } m = 1, 2, 3, \cdots \tag{2.21}$$

Note that the rigid body mode possesses kinetic energy only.

The Lagrangian for the system is given by

$$L \equiv T - U \tag{2.22}$$

Lagrange's equations of motion may be written as [8]

$$\frac{d}{dt}\left(\frac{\partial L}{\partial \dot{q}_i}\right) - \frac{\partial L}{\partial q_i} = F_i \text{ for } i = 0, 1, 2, \cdots \tag{2.23}$$

where F_i is the generalised force related to i th mode shape function and the generalised coordinate q_i, which is a non-conservative force resulting from external forces or moments. As orthogonality between the mode shape functions exists, as presented in equations (2.16), (2.17), (2.19) and (2.21), substituting equations (2.18), (2.20) and (2.22) into (2.23) gives a simple form for the modal equation of motion.

$$M_m^b \ddot{q}_m + K_m^b q_m = F_m \text{ for } m = 0, 1, 2, 3, \cdots \tag{2.24}$$

where the generalised force F_m is also a function of time and defined by [12]

$$F_m(t) = \int_0^{L_x} f(x,t)\phi(x)dx\,. \tag{2.25}$$

Assuming harmonic motion of frequency ω and introducing the external point force $F_0\delta(x-x_1)$, the force function shown in equation (2.25) becomes (using complex notation)

$$\tilde{f}(x,t) = F_0\delta(x-x_1)e^{i\omega t}\,. \tag{2.26}$$

where x_1 is the coordinate where the force is applied. This gives $\tilde{F}_m(t) = F_0\phi(x_1)e^{i\omega t}$. Then from equation (2.24) the steady state solution for the generalised coordinate $\tilde{q}_m$ is [11]

$$\tilde{q}_m = \frac{\tilde{F}_m}{M_m^b\left(\omega_m^2 - \omega^2\right)} \tag{2.27}$$

where $\tilde{F}_m$ is the harmonic force corresponding to the generalised coordinate $\tilde{q}_m$ and the natural frequency ω_m is related to the modal mass and stiffness by

$$\omega_m^2 = \frac{K_m^b}{M_m^b}\,. \tag{2.28}$$

Alternatively, as the relevant wavenumbers are given in equation (2.13) the natural frequencies ω_m can be obtained from equation (2.3)

$$\omega_m^2 = k_x^4 \frac{D_b}{m_b'} \text{ for } m = 0,1,2,\cdots \tag{2.29}$$

where $m = 0$ represents the rigid body mode for the sliding boundary condition considered.

2.3 Introduction of hysteretic damping

If structural damping is introduced to the beam, the bending stiffness is given by

$$\tilde{D}_b = D_b\left(1 + i\eta_b\right) \tag{2.30}$$

where η_b is structural loss factor. Then, equations (2.27), (2.28) and (2.29) are changed to include the damping in the structure as follows.

$$\tilde{q}_m = \frac{\tilde{F}_m}{M_m^b\left[\omega_m^2\left(1+i\eta_b\right)-\omega^2\right]} \tag{2.31}$$

and

$$\tilde{\omega}_m^2 = k_x^4 \frac{\tilde{D}_b}{m_b'} \tag{2.32}$$

i.e. a complex generalised stiffness is introduced for simplicity.

3. A MODAL DESCRIPTION FOR PLATE VIBRATION

3.1 Equation of motion based on a modal expansion

Similar to equation (2.1), the flexural displacement of a structure such as a plate having an arbitrary shape can also be represented using an infinite series as

$$w_p(x,y,t) = \sum_r \psi_r(x,y)\, q_r(t) \tag{3.1}$$

where $\psi_r(x,y)$ is a mode shape function of the plate, $q_r(t)$ is the corresponding generalised coordinate.

Limiting the plate to a rectangular shape, its mode shape can be represented by combination of mode shapes of the two directions. Thus, the mode shape of the rectangular plate $\psi_r(x,y)$ can be expressed as the product of two separable functions so that each depends on a single spatial variable x or y i.e.

$$\psi_r(x,y) = \phi_{m_r}(x)\phi_{n_r}(y) = \phi_{m_r}\phi_{n_r} \tag{3.2}$$

where $\phi_{m_r}(x)$ and $\phi_{n_r}(y)$ are selected as two linearly independent sets satisfying all the appropriate boundary conditions. Thus, this separation of variables may only be applicable to this kind of rectangular plate analysis. In the present report, mode shape functions of vibrating beams are chosen, which was introduced by Vlasov (see Szilard [9]). In general, the separable solution is an approximate approach as it is only in the special cases where a pair of opposite parallel edges are either simply supported or sliding that the governing equation of motion for the plate can be solved exactly by this type of separable expansion.

If all edges of the rectangular plate are sliding then the corresponding exact mode shape functions are

$$\phi_{m_r} = \cos k_x x\,,\ \phi_{n_r} = \cos k_y y \tag{3.3}$$

where

$$\begin{aligned} k_x &= m_r\pi/L_x \ \text{ for } m_r = 0,1,2,\cdots \\ k_y &= n_r\pi/L_y \ \text{ for } n_r = 0,1,2,\cdots. \end{aligned} \tag{3.4}$$

Orthogonality of the shape functions holds in this case, i.e.

$$\int_0^{L_x}\int_0^{L_y}\psi_r\psi_s dxdy = 0 \text{ for } r \neq s \tag{3.5}$$

where a mode number s is introduced to distinguish from a mode number r.

Making use of orthogonality of the mode shape, the kinetic energy T of the rectangular plate is given by

$$T = \frac{1}{2}\sum_r M_r^p \dot{q}_r^2 \tag{3.6}$$

where the modal mass of the plate is defined by

$$M_r^p = \int_0^{L_y}\int_0^{L_x} m_p'' \psi_r^2 dxdy \tag{3.7}$$

As the mode shape function ψ_r is given by two separable functions, equation (3.7) is simply

$$M_r = \int_0^{L_y}\int_0^{L_x} m_p''\left(\phi_{m_r}\phi_{n_r}\right)^2 dxdy = m_p''\int_0^{L_x}\phi_{m_r}^2 dx\int_0^{L_y}\phi_{n_r}^2 dy \tag{3.8}$$

Note that the integrals are $L/2$ for m_r, $n_r \geq 1$ and L for m_r, $n_r = 0$. The strain energy U of the rectangular plate is

$$U = \frac{D_p}{2}\int_0^{L_y}\int_0^{L_x}\left[\left(\frac{\partial^2 w_p}{\partial x^2}\right)^2 + \left(\frac{\partial^2 w_p}{\partial y^2}\right)^2 + 2\nu\frac{\partial^2 w_p}{\partial x^2}\frac{\partial^2 w_p}{\partial y^2} + 2(1-\nu)\left(\frac{\partial^2 w_p}{\partial x \partial y}\right)^2\right]dxdy . \tag{3.9}$$

Similar to the modal mass, substituting equation (3.1) and (3.2) into equation (3.9) results in

$$U = \frac{1}{2}\sum_r K_r^p q_r^2 . \tag{3.10}$$

where the modal stiffness of the rectangular plate K_r^p is

$$K_r^p = D_p\int_0^{L_y}\int_0^{L_x}\left[\phi_{n_r}^2\left(\frac{\partial^2\phi_{m_r}}{\partial x^2}\right)^2 + \phi_{m_r}^2\left(\frac{\partial^2\phi_{n_r}}{\partial y^2}\right)^2 + 2\nu\phi_{m_r}\phi_{n_r}\frac{\partial^2\phi_{m_r}}{\partial x^2}\frac{\partial^2\phi_{n_r}}{\partial y^2} + 2(1-\nu)\left(\frac{\partial\phi_{m_r}}{\partial x}\frac{\partial\phi_{n_r}}{\partial y}\right)^2\right]dxdy \tag{3.11}$$

Inserting the mode shape functions shown in equation (3.3) gives a simple form of equation (3.11) as

$$K_r^p = D_p \frac{L_x L_y}{2}\left[\left(\frac{m_r\pi}{L_x}\right)^2 + \left(\frac{n_r\pi}{L_y}\right)^2\right]^2 \quad \text{for } m_r = 0 \text{ or } n_r = 0$$

$$K_r^p = D_p \frac{L_x L_y}{4}\left[\left(\frac{m_r\pi}{L_x}\right)^2 + \left(\frac{n_r\pi}{L_y}\right)^2\right]^2 \quad \text{for otherwise.} \tag{3.12}$$

Therefore, the equation of motion using Lagrange's equation (2.23) is simply found as

$$M_r^p \ddot{q}_r + K_r^p q_r = F_r, \tag{3.13}$$

where the generalised force for the rectangular plate is defined by

$$F_r = \int_0^{L_x}\int_0^{L_y} f(x,y,t)\psi_r(x,y)\,dxdy = \int_0^{L_x}\int_0^{L_y} f(x,y,t)\phi_{m_r}\phi_{n_r}\,dxdy\,. \tag{3.14}$$

In particular, if a point force with complex amplitude $\tilde{F}_0$ is applied at an arbitrary position $(x,y) = (x_1, y_1)$ then the generalised force amplitude will be

$$\tilde{F}_r = \int_0^{L_x}\int_0^{L_y} \tilde{F}_0\delta(x-x_1)\delta(y-y_1)\phi_{m_r}\phi_{n_r}\,dxdy = \tilde{F}_0\phi_{m_r}(x_1)\phi_{n_r}(y_1)\,. \tag{3.15}$$

Similar to the beam in the previous section, assuming harmonic motion at frequency ω and introducing structural damping to the plate results in

$$\tilde{q}_r = \frac{\tilde{F}_r}{M_r^p\left[\omega_r^2\left(1+i\eta_p\right)-\omega^2\right]} \tag{3.16}$$

where η_p is the structural loss factor of the plate and $\omega_r^2 = K_r^p / M_r^p$.

4. A MODAL FORMULATION FOR THE COUPLED MOTION OF A SYSTEM OF TWO OR FOUR BEAMS ATTACHED TO A PLATE

4.1 Framed structure

The motion of a framed structure consisting of four beams and a rectangular plate, as shown in Figure 1, is investigated here. The motion of the uncoupled beam and the plate can be represented using the mode shape functions described previously. Similarly, for the framed structure, its behaviour can be described in terms of mode shapes and Lagrange's equations of motion can be derived based on energy relationships. It does not seem necessary to obtain a mode of the framed structure itself, as the relevant modal matrices of the uncoupled structures are already presented in sections 2 and 3. Thus, in the present report the motion of the built-up structure is obtained by the *coupling* technique and how the matrices of the uncoupled structures are coupled will be explained.

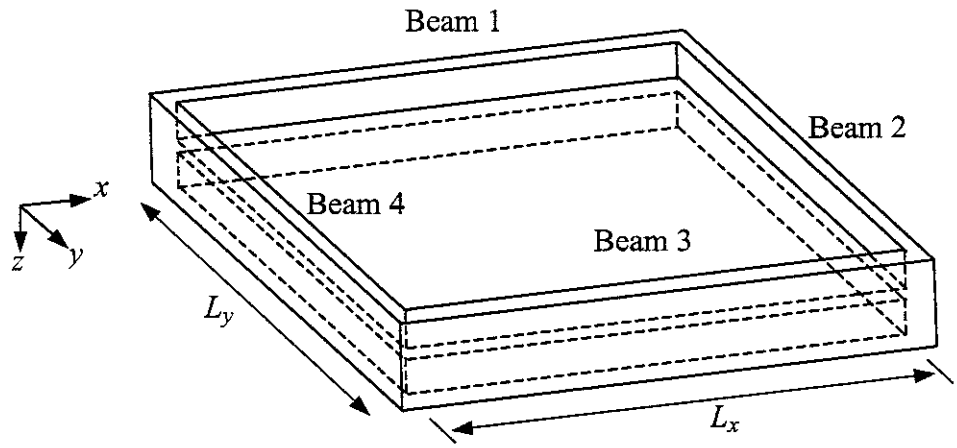

Figure 1. The coupled structure consisting of four beams and a rectangular plate.

For simplicity, the beams are assumed infinitely stiff to torsion and correspondingly all edges of the plate are assumed to be sliding (rotation is restrained through rigid coupling to the corresponding beam). Similar to the uncoupled plate, it is assumed in the following that the plate response is given using a separable solution. Thus, the two sets of functions in the two directions correspond to the mode shape functions of the corresponding beams along the edges with their ends sliding.

As explained in section 3.1, this method using the separation of the variables is an approximate method for general boundary conditions as characteristic functions and/or their derivatives are not always orthogonal [9, section 2.6]. The general form of the function is shown in equation (2.2) the coefficients of which should be determined from the boundary conditions. Some particular boundary conditions such as sliding edges considered here give an exact solution (apart from truncation to a finite number of mode shape functions).

4.2 Solution in terms of generalised coordinates

The flexural displacement of the plate with four beams attached can be written as a sum over a set of functions that span the motion and satisfy the boundary conditions. The mode shapes of the uncoupled plate are suitable for this. Thus

$$w_p(x,y,t) = \sum_r \psi_r(x,y) q_r(t) \tag{4.1}$$

where ψ_r are the r th mode shapes of the uncoupled plate and q_r are generalised coordinates. The displacement of the beams shown in Figure 1 are given by

$$\begin{aligned} w_{b1}(x,t) &= w_p(x,0,t);\ w_{b3}(x,t) = w_p(x,L_y,t) \\ w_{b4}(y,t) &= w_p(0,y,t);\ w_{b2}(y,t) = w_p(L_x,y,t) \end{aligned} \tag{4.2}$$

due to continuity at the plate edges.

It is convenient to write equation (4.1) in matrix form

$$w_p(x,y,t) = \boldsymbol{\Psi}\mathbf{q} \tag{4.3}$$

where

$$\boldsymbol{\Psi} = \begin{bmatrix} \psi_1 & \psi_2 & \cdots & \psi_R \end{bmatrix} \tag{4.4}$$

and

$$\mathbf{q} = \begin{bmatrix} q_1 & q_2 & \cdots & q_R \end{bmatrix}^T \tag{4.5}$$

Although, strictly, the summation in equation (4.1) should be over an infinite number of terms, for practical reasons these are truncated. The maximum mode number R is chosen after various simulations to check convergence.

From equation (3.2) of section 3 the mode shapes of the plate are

$$\psi_r(x,y) = \phi_{m_r}(x)\phi_{n_r}(y) \tag{4.6}$$

where

$$\begin{aligned} \phi_{m_r}(x) &= \cos k_x x, \;\; k_x = m_r\pi/L_x \\ \phi_{n_r}(y) &= \cos k_y y, \;\; k_y = n_r\pi/L_y \end{aligned} \tag{4.7}$$

Thus, maximum mode number of the plate $r = R$ is expressed in terms of the beam mode number $m_r n_r = MN$.

From equations (4.1) and (4.2) the kinetic energy of the plate and beams can be evaluated in terms of the generalised coordinate, q_r. For the plate

$$T_p = \frac{m_p''}{2}\int_0^{L_y}\int_0^{L_x}\left(\frac{\partial w_p}{\partial t}\right)^2 dxdy\,. \tag{4.8}$$

Therefore

$$T_p = \frac{m_p''}{2}\sum_r\sum_s\int_0^{L_x}\int_0^{L_y}\psi_r\psi_s\dot{q}_r\dot{q}_s dxdy \tag{4.9}$$

which can be written in the form

$$T_p = \frac{1}{2}\dot{\mathbf{q}}^T\mathbf{M}_p\dot{\mathbf{q}} \tag{4.10}$$

with

$$M_{rs}^p = m_p''\int_0^{L_x}\int_0^{L_y}\psi_r\psi_s dxdy\,. \tag{4.11}$$

where subscripts r and s are the corresponding mode numbers producing M^p and

$$\psi_s(x,y) = \phi_{m_s}(x)\phi_{n_s}(y)\,. \tag{4.12}$$

Note that the subscripts r and s can also be used to indicate location of the r th row and s th column in matrix $\mathbf{M}_p$ for convenience whereas subscripts m_r, m_s, n_r and n_s are used to describe the mode number of the beam functions used in the expansion, related to modes r and s.

Since ψ_r is the mode shape of the uncoupled plate, $\mathbf{M}_p$ is equal to the modal mass matrix of the uncoupled plate,

$$M_{rs}^{p} = \begin{cases} M_r^p & \text{for } r = s \\ 0 & \text{for otherwise} \end{cases}. \tag{4.13}$$

For beam 1 $(y = 0)$, the kinetic energy can be written

$$T_{b1} = \frac{m'_{b1}}{2}\int_0^{L_x}\left(\frac{\partial w_{b1}}{\partial t}\right)^2 dx = \frac{m'_{b1}}{2}\int_0^{L_x}\left(\frac{\partial w_p}{\partial t}\right)^2_{y=0} dx. \tag{4.14}$$

Substituting from equations (4.1), (4.6) and (4.12) results in the expression of the beam kinetic energy in terms of shape functions used in the modal expansion for the plate which provides, through continuity, the displacement of the beams.

$$T_{b1} = \frac{m'_{b1}}{2}\sum_r\sum_s\int_0^{L_x}\phi_{m_r}(x)\phi_{m_s}(x)dx\,\phi_{n_r}(0)\phi_{n_s}(0)\dot{q}_r\dot{q}_s. \tag{4.15}$$

Now $\phi_{n_r}(0) = \phi_{n_s}(0) = 1$, and from orthogonality of the ϕ_m,

$$\int_0^{L_x} m'_{b1}\phi_{m_r}(x)\phi_{m_s}(x)dx = \begin{cases} M_{m_r}^{b1} & \text{for } m_r = m_s \\ 0 & \text{for } m_r \neq m_s \end{cases}. \tag{4.16}$$

So T_{b1} can be written in terms of a generalised mass matrix

$$T_{b1} = \frac{1}{2}\dot{\mathbf{q}}^T\mathbf{M}_{b1}\dot{\mathbf{q}} \tag{4.17}$$

with

$$M_{rs}^{b1} = M_{m_r}^{b1}\delta_{m_r m_s} \tag{4.18}$$

where r and s indicate the location of M_{rs}^{b1} in matrix $\mathbf{M}_{b1}$ and $\delta_{m_r m_s}$ is the Kronecker delta. Similarly for beam 4 $(x = 0)$ the generalised mass matrix is found as

$$M_{rs}^{b4} = M_{n_r}^{b4}\delta_{n_r n_s} \tag{4.19}$$

while for beams 3 and 2 ($y = L_y$ and $x = L_x$)

$$M_{rs}^{b3} = M_{m_r}^{b3}\delta_{m_r m_s}(-1)^{n_r}(-1)^{n_s} \tag{4.20}$$

$$M_{rs}^{b2} = M_{n_r}^{b2}\delta_{n_r n_s}(-1)^{m_r}(-1)^{m_s} \tag{4.21}$$

where use is made of $\cos n\pi = (-1)^n$.

The total kinetic energy of the coupled system can be written as

$$\begin{aligned} T &= T_p + T_{b1} + T_{b2} + T_{b3} + T_{b4} \\ &= \frac{1}{2}\dot{\mathbf{q}}^T \mathbf{M}\dot{\mathbf{q}} \end{aligned} \tag{4.22}$$

where $\mathbf{M}$ is the generalised mass matrix given by

$$\mathbf{M} = \mathbf{M}_p + \mathbf{M}_{b1} + \mathbf{M}_{b2} + \mathbf{M}_{b3} + \mathbf{M}_{b4} \tag{4.23}$$

with $\mathbf{M}_p$, $\mathbf{M}_{b1}$, $\mathbf{M}_{b2}$, $\mathbf{M}_{b3}$ and $\mathbf{M}_{b4}$ given by equations (4.13) and (4.18) - (4.21). Note that while $\mathbf{M}_p$ is diagonal $\mathbf{M}_{bi}$ is not, so that the plate modes are coupled through the generalised mass matrix.

Similarly, the generalised stiffness matrix can be found from the strain energy of the coupled structure. The plate potential energy is given by equations (3.9) and (4.1) as

$$U_p = \frac{D_p}{2}\sum_r \int_0^{L_y}\int_0^{L_x}\left[\left(\frac{\partial^2\psi_r}{\partial x^2}\right)^2 + \left(\frac{\partial^2\psi_r}{\partial y^2}\right)^2 + 2\nu\frac{\partial^2\psi_r}{\partial x^2}\frac{\partial^2\psi_r}{\partial y^2} + 2(1-\nu)\left(\frac{\partial^2\psi_r}{\partial x \partial y}\right)^2\right] q_r^2\, dxdy \tag{4.24}$$

which, in matrix form, is

$$U_p = \frac{1}{2}\mathbf{q}^T \mathbf{K}_p \mathbf{q}. \tag{4.25}$$

The modal stiffness in $\mathbf{K}_p$ is the same as that of the uncoupled plate, which is

$$K_{rs}^p = \begin{cases} K_r^p & \text{for } r = s \\ 0 & \text{for otherwise} \end{cases}. \tag{4.26}$$

where K_r^p is already shown in equation (3.12). It can also be found simply from the natural frequencies of the plate and the modal mass as

$$K_r^p = \omega_{p,r}^2 M_r^p . \tag{4.27}$$

For beam 1 $(y = 0)$, the strain energy is

$$U_{b1} = \frac{D_b}{2} \int_0^{L_x} \left(\frac{\partial^2 w_b}{\partial x^2} \right)^2 dx = \frac{D_b}{2} \int_0^{L_x} \left(\frac{\partial^2 w_p}{\partial x^2} \right)_{y=0}^2 dx . \tag{4.28}$$

Substituting equations (4.1), (4.6) and (4.12) in equation (4.28) gives

$$U_{b1} = \frac{D_b}{2} \sum_r \sum_s \phi_{n_r}(0) \phi_{n_s}(0) q_r q_s \int_0^{L_x} \frac{\partial^2 \phi_{m_r}(x)}{\partial x^2} \frac{\partial^2 \phi_{m_s}(x)}{\partial x^2} dx . \tag{4.29}$$

Thus, orthogonality of the beam mode shape function ϕ_m gives

$$\int_0^{L_x} \frac{\partial^2 \phi_{m_r}(x)}{\partial x^2} \frac{\partial^2 \phi_{m_s}(x)}{\partial x^2} dx = \begin{cases} K_{m_r}^{b1} & \text{for } m_r = m_s \\ 0 & \text{for } m_r \neq m_s \end{cases} . \tag{4.30}$$

Now $\phi_{n_r}(0) = \phi_{n_s}(0) = 1$ and the strain energy can be described as

$$U_{b1} = \frac{1}{2} \mathbf{q}^T \mathbf{K}_{b1} \mathbf{q} \tag{4.31}$$

where the terms of stiffness matrix $\mathbf{K}_{b1}$ are

$$K_{rs}^{b1} = K_{m_r}^{b1} \delta_{m_r m_s} . \tag{4.32}$$

For beam 4 $(x = 0)$ the generalised matrix is found as

$$K_{rs}^{b4} = K_{n_r}^{b4} \delta_{n_r n_s} . \tag{4.33}$$

Similarly for beams 3 and 2 ($y = L_y$ and $x = L_x$)

$$K_{rs}^{b3} = K_{m_r}^{b3} \delta_{m_r m_s} (-1)^{n_r} (-1)^{n_s} \tag{4.34}$$

$$K_{rs}^{b2} = K_{n_r}^{b2} \delta_{n_r n_s} (-1)^{m_r} (-1)^{m_s} \tag{4.35}$$

where $(-1)^m$ is used for $\cos m\pi$.

The strain energy of the coupled system can be written as

$$U = U_p + U_{b1} + U_{b2} + U_{b3} + U_{b4}$$
$$= \frac{1}{2}\mathbf{q}^T\mathbf{K}\mathbf{q} \tag{4.36}$$

where the generalised stiffness matrix $\mathbf{K}$ is

$$\mathbf{K} = \mathbf{K}_p + \mathbf{K}_{b1} + \mathbf{K}_{b2} + \mathbf{K}_{b3} + \mathbf{K}_{b4} \tag{4.37}$$

where the corresponding equations of the matrices are given by equations (4.26) and (4.32) - (4.35) respectively. Similar to the mass matrix only $\mathbf{K}_p$ is diagonal.

The corresponding generalised force vector representing the external force is given by

$$\mathbf{F} = \begin{bmatrix} F_1 & F_2 & \cdots & F_R \end{bmatrix}^T \tag{4.38}$$

where each factor F_r is the generalised force corresponding to the plate mode shape r and can also be expressed in terms of a beam mode number $m_r n_r$. Thus for a point force in particular as shown in equation (3.15) it is given as

$$F_r = F_0 \phi_{m_r}(x_1)\phi_{n_r}(y_1) \tag{4.39}$$

where F_0 is the amplitude of the point force applied at $x = x_1$ and $y = y_1$.

Assuming steady state harmonic motion and introducing the hysteretic damping to the system, the generalised coordinates can be obtained from the generalised mass, stiffness matrix and the force matrix as follows.

$$\tilde{\mathbf{q}} = \left(\tilde{\mathbf{K}} - \omega^2\mathbf{M}\right)^{-1}\tilde{\mathbf{F}}. \tag{4.40}$$

where structural damping has been included in the matrix $\tilde{\mathbf{K}}$ according to the structural damping of each subsystem. Finally the response of the coupled structure can be found from equation (4.1).

4.3 Numerical results

In this section, numerical simulations are presented. The structure consisting of four beams and a rectangular plate shown in Figure 1 was investigated. The ends of the four beams are assumed to be in sliding conditions and the torsional stiffness of the beams is assumed infinite. Accordingly, the edges of the plate are also assumed to be in sliding conditions.

The numerical analysis based on the wave method will also be included later. An important assumption of the wave method used in the present report is that the wavenumber of the free plate should be at least twice as large as the free beam wavenumber. This requirement leads to having the height of the beam and the thickness of the plate chosen so that the ratio of the free wavenumber of the subsystems is at least 2. In principle this is not a restriction on the modal approach, but has been adopted so as to be able to consider results produced by the two methods. The material properties and dimensions of the coupled structure are given in Table 1 and the free wavenumbers of the beam and the plate are compared in Figure 2. The corresponding wavenumber ratio is a constant and equal to $k_p/k_b = 3.18$. This is large enough to apply the wave method.

Table 1. Material properties and dimensions of the coupled structure shown in Figure 1.

Material	Perspex
Young's modulus, E (GNm^{-2})	4.4
Poisson's ratio, ν	0.38
Density, ρ (kgm^{-3})	1152.0
Beam length, L_x (m)	1.0
Beam thickness, t_b (mm)	6.0
Plate width, L_y (m)	0.75
Plate thickness, t_p (mm)	2.0
Height of the beam, h (mm)	22.0
DLF of the beam, η_b	0.05
DLF of the plate, η_p	0.05

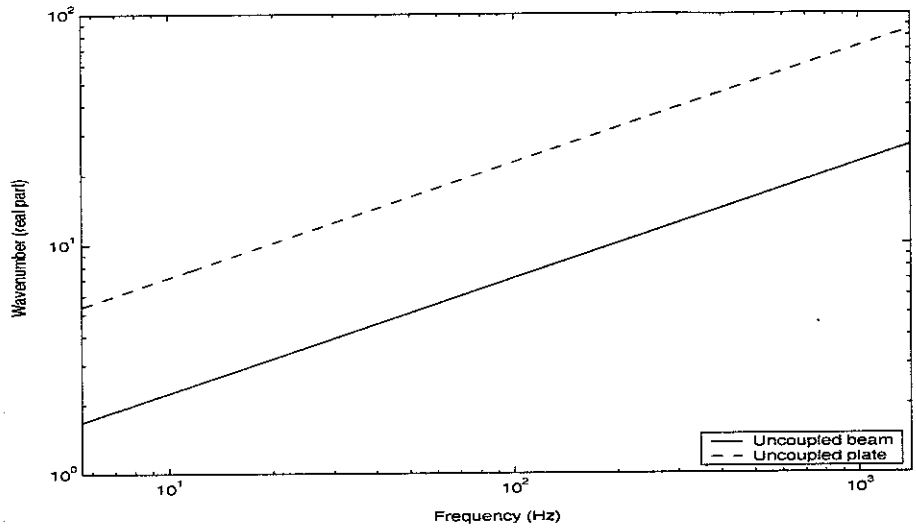

Figure 2. Wavenumbers of the uncoupled subsystems.

4.3.1 Two-beam-plate coupled system: test of convergence

As explained in section 4.2, an exact answer based on the modal method requires that all possible vibrational modes are included. However, this is impractical in a real application and the number of modes to be included in the numerical solution is an important concern. Thus, firstly the difference in response predictions between the modal method and other known numerical analyses was investigated. Comparing the difference between two methods, it is expected that the appropriate number of modes necessary for the frequency range of interest (5.6 - 1412 Hz) can be ascertained. In this frequency range, the stiffer beam has a small number of modes while the plate has a large number of flexural modes so that the problem is representative of a mid-frequency problem.

Previously the Fourier technique was introduced to find the response of the coupled structure consisting of two beams and a rectangular plate [13] and the results of this technique can be used for initial comparison. It can be expected that the number of modes required for the two-beam structure can also be used reliably for the equivalent four-beam structure of similar dimensions. The four-beam structure is actually stiffer than the two-beam case suggesting that fewer modes should be required.

The two-beam structure considered is shown in Figure 3. All material properties and dimensions are the same as for the four-beam structure. Also the sliding boundary conditions as described previously were assumed. The relevant matrix equations are shown in section 4.2. For example, the total mass matrix of the coupled structure is given by equation (4.23).

However, as there is no beams along the y direction, the corresponding mass and stiffness beam contributions should be zero.

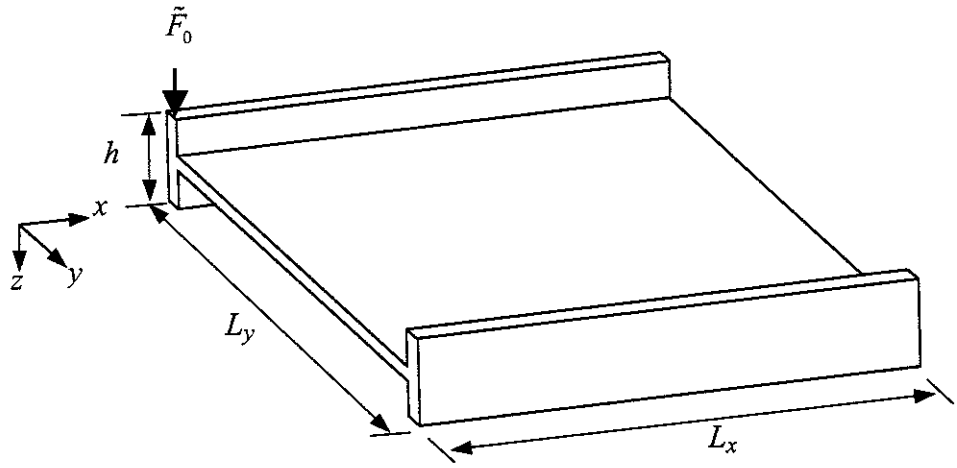

Figure 3. A built-up structure consisting of two finite beams attached to a rectangular plate.

In the Fourier approach the accuracy of the response is dependent on the wavenumber range considered in the calculation. As previously [13], this is defined in terms of the non-dimensional wavenumber, given by

$$\gamma_{b,x} = k_x / k_b \tag{4.41}$$

where $k_x = n\pi / L_x$ is the real wavenumber defined in the spatial Fourier transform, n is the number of half-cosine waves along the beam length L_x and $k_b^4 = m_b' \omega^2 / D_b$, where m_b' is the mass per unit length, ω is frequency and D_b is the bending stiffness of the beam. Clearly extending the range for the Fourier transform produces better results. However, it also requires much more computation time and it was shown that a range of $\gamma = \pm 15$ results in less than 0.01% error at 10, 100 and 1000 Hz for the present coupled structure [13]. Thus, in the present report, the non-dimensional wavenumber range of $\gamma = \pm 15$ was chosen, which corresponds to $n = 128$ at 1412 Hz.

An external unit force is applied at $x = 0$ of beam 1 as shown in Figure 3. To obtain the estimate of the space-averaged kinetic energy of the plate, 20 random points are selected. Then this averaged kinetic energy is used for comparing the difference between the two methods, namely the Fourier technique and the modal method. The difference is given as an error in dB, assuming the Fourier technique is an exact result for this problem.

$$e(\mathrm{dB}) = 10\log_{10}\overline{E}_{\omega} \tag{4.42}$$

where $\overline{E}_{\omega}$ is the frequency-averaged difference between the two methods normalised by the Fourier estimate and defined by

$$E_{\omega} = E(\omega) = \left|\left\langle T_{p,F}(\omega)\right\rangle - \left\langle T_{p,M}(\omega)\right\rangle\right| \Big/ \left\langle T_{p,F}(\omega)\right\rangle \tag{4.43}$$

where $\left\langle T_{p,F}(\omega)\right\rangle$ is the space-averaged kinetic energy of the plate based on the Fourier technique and $\left\langle T_{p,M}(\omega)\right\rangle$ is that based on the modal method.

The difference e is evaluated when the maximum mode number in the x direction (M) and the maximum mode number in the y direction (N) considered in the calculation are changed. For the case when the frequency covers 5.6 - 1412 Hz, the variation in the difference is given in Figure 4. To reduce calculation time the mode numbers were chosen to be at intervals equal to 5.

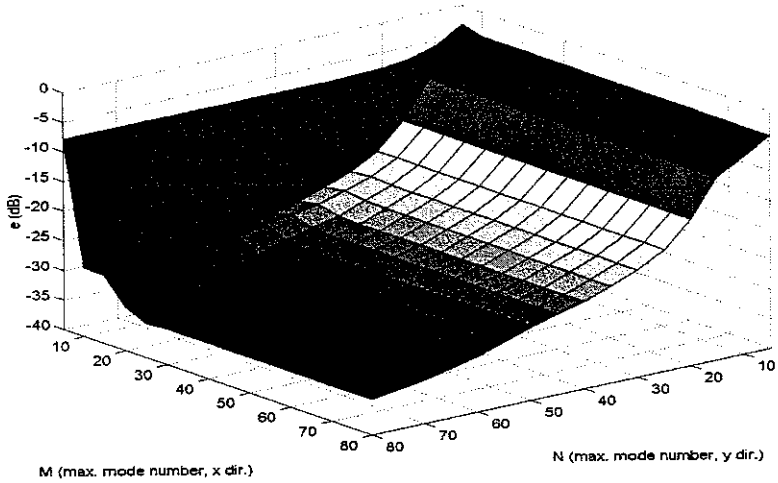

Figure 4. Error in the modal method compared to the Fourier technique as a function of the number of modes used (Frequency of interest 5.6 - 1412 Hz).

It can be seen that the space and frequency-averaged difference reduces with increasing number of modes considered in the calculations. It is interesting to compare the slope of the surface in the x direction and the y direction. In the y direction the difference gradually reduces with increasing mode number. However, in the x direction the difference suddenly reduces at small mode number, which is about 9. This corresponds to the beam wavenumber at 1412 Hz ($k_b = 26.7$ rad/m). One can see that this is because there are two stiffer beams

lying in the x direction which are the dominant influence on the motion in this direction. However the beams lying in the x direction do not appear to influence so strongly the motion with respect to the y direction and it appears that one needs a higher number of sliding modes in the y direction to get a good prediction.

Although the tendency in the error can be identified, the interval of 5 used appears too coarse and the calculation was repeated using an interval of 2. A contour plot of the resulting error is shown in Figure 5. It can be seen that the difference reduces for a small number of modes in the x direction rather than the y direction. This can be distinguished by the black thicker line (dashed), which is at about -15 dB or about 3 % difference. The value of about -25 dB indicated by the black thicker line (solid) is about 0.3 %. The averaged error of 0.3 % occurs for example when the maximum mode numbers $M = 18$ and $N = 40$ are considered ($e = 0.3\%$).

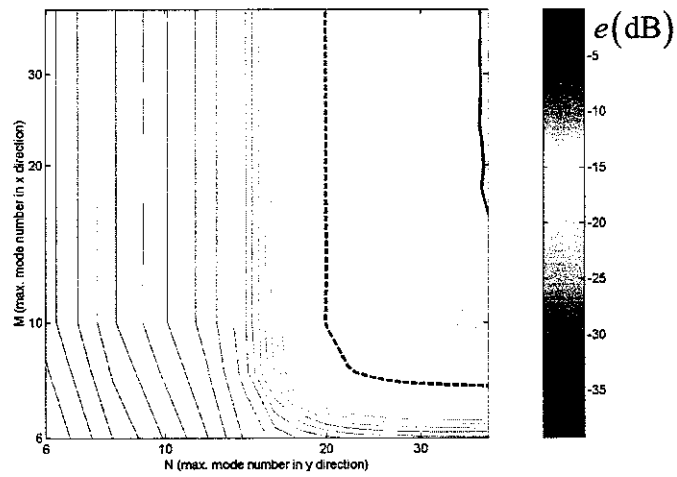

Figure 5. Contours of the error as a function of the numbers of modes in the modal solution (Frequency of interest 5.6 - 1412 Hz).

The error is clearly related to the mode numbers, and for obtaining the response at a specified accuracy the number of modes to be included depends upon the dimensions and physical properties of the structure. Thus, it seems useful to introduce a quantity less influenced by the dimensions instead of the mode number and one can think that a normalised wavenumber might be a good alternative. The normalised wavenumbers are given by

$$\gamma_{p,x} = k_x / k_{p,\max} = M\pi / \left(L_x k_{p,\max} \right), \; \gamma_{p,y} = k_y / k_{p,\max} = N\pi / \left(L_y k_{p,\max} \right) \qquad (4.44)$$

where M and N are the maximum mode number considered in the x and y direction respectively, L_x is the length of the beam, L_y is the width of the plate and $k_p^4 = m_p'' \omega^2 / D_p$ is the plate free wavenumber and maximum value $k_{p,\max}$ is obtained from the maximum frequency considered. The averaged error e in Figure 4 is replotted in Figure 6 with respect to the non-dimensional wavenumbers. The non-dimensional wavenumbers corresponding to the maximum mode number $M = 18$ and $N = 40$ are $\gamma_{p,x} = 0.66$ and $\gamma_{p,y} = 1.97$ respectively when the averaged difference is 0.3 %.

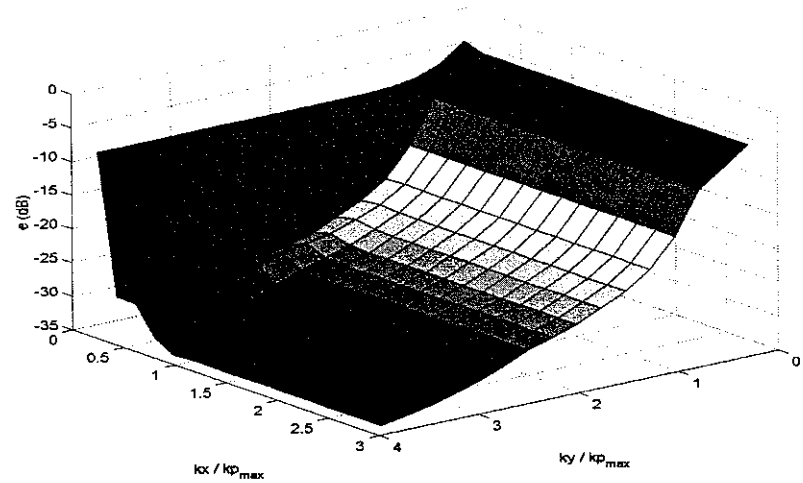

Figure 6. Difference distribution in terms of normalised mode numbers (Frequency of interest is 5.6 - 1412 Hz).

Note that the results shown in Figures 4 - 6 are obtained for a frequency range 5.6 - 1412 Hz. It is clear that the averaged error e varies according to the frequency range. The same investigation represented by Figures 4 - 6 was repeated for different frequency ranges and the results summarised in Table 2.

Table 2. The relationship between the averaged error e, mode number, non-dimensional wavenumber and frequency range.

	$M \times N$	$\gamma_{p,x} \times \gamma_{p,y}$	$e(\%)$
5.6 - 1412 Hz	18×40	0.66×1.97	0.30
5.6 - 708 Hz	14×34	0.73×2.36	0.28
5.6 - 355 Hz	12×28	0.88×2.74	0.29

Although it is clear that more accurate modal results need more modes, much more computational time is also necessary for such accuracy. Thus, an appropriate maximum mode number should be selected. Note that for the frequency range 5.6 - 1412 Hz in Table 2 there is no unique value to meet the condition $e \leq 0.3$ %. However, as mentioned in section 4.3 the wavenumber ratio of the uncoupled system k_p/k_b is 3.18 in the present case. Thus it seems reasonable to choose the maximum mode numbers so that the corresponding trace wavenumbers have the similar ratio as

$$k_y^2 = k_p^2 - k_x^2 = k_p^2 - k_b^2 = k_p^2\left(1 - k_b^2/k_p^2\right) \approx k_p^2. \tag{4.45}$$

The maximum mode numbers chosen in Table 2 approximately follow the relationship of equation (4.45). Also for the four-beam coupled structure, the accuracy may increase as two other beams are attached to the two-beam coupled structure when these beams are stiffer than the plate and hence govern the coupled structural behaviour. Thus, it is expected that if $M \geq 40$ and $N \geq 40$ then the error will be less than 0.3 % ($e < 0.3$ %). Subsequently in the present report $M = 40$ and $N = 40$ have been chosen for computations as the computational time is acceptable. These correspond to a maximum plate wavenumber of twice the free plate wavenumber at the maximum frequency (and six times that of the beams).

4.3.2 Four-beam-plate coupled system

The four-beam structure shown in Figure 1 is analysed using the procedure represented in section 4.2. Firstly the point mobility of the coupled structure is obtained when a harmonic point force of unit magnitude is applied at $x = 0$, $y = 0$, the joint of beams 1 and 4. The response is compared with a finite element (FE) model prediction in Figure 7. The beam in the FEM is modelled using Euler-Bernoulli beam elements (400 elements) and the plate with shell elements (9804 elements) corresponding to at least 8 elements per plate free wavelength ($\lambda_p = 0.074$ m at 1412 Hz) and the sliding conditions of all plate edges and the ends of the beams are also assumed. The result of the modal method shows an excellent agreement with that of the FE model, the latter itself also being an approximate numerical solution.

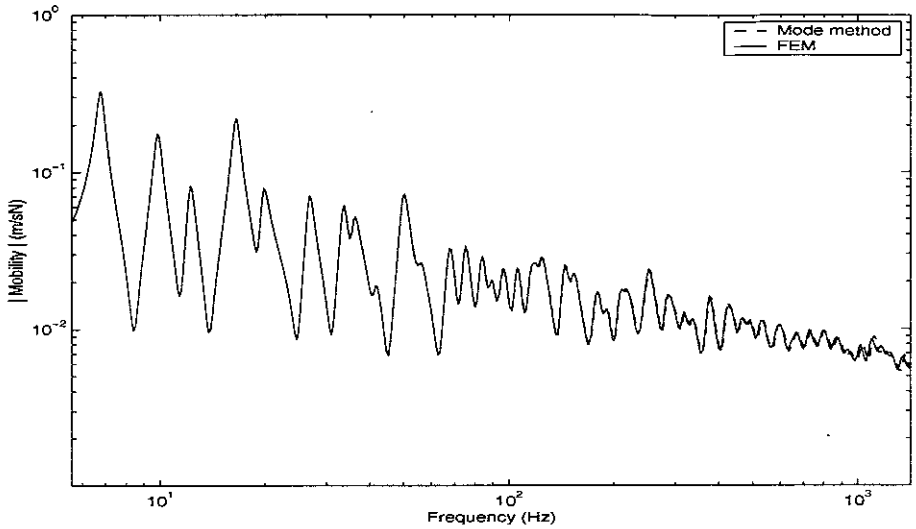

Figure 7. Point mobility comparison between the modal method and the FE (excitation at $x = 0$).

Also an example of the transfer mobility comparison with FE is shown in Figure 8, also giving good agreement.

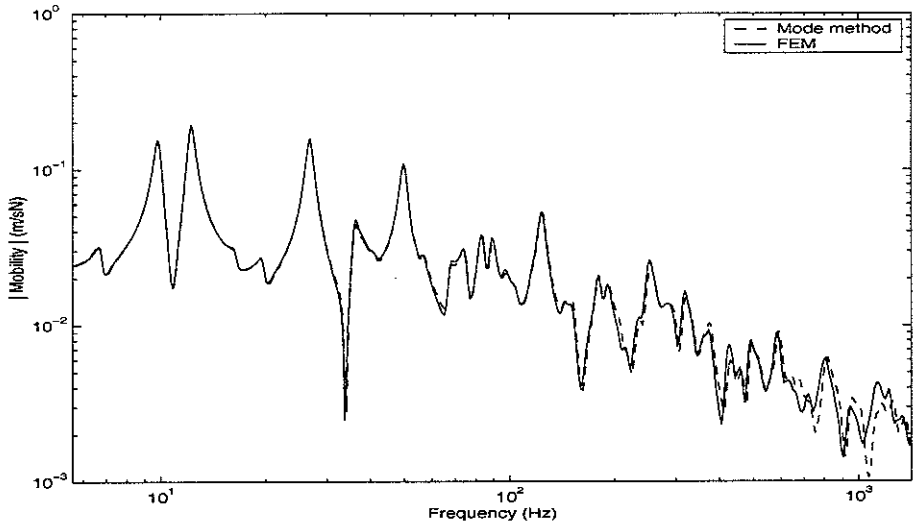

Figure 8. Transfer mobility comparison between the modal method and the FE (excitation at $x = 0$, response at $x = 0.51$, $y = 0.51$).

The power balance between subsystems should hold and the dissipated powers of subsystems were used to investigate the power balance relationship. The dissipated power of the subsystem can be found from the maximum strain energy of the subsystem. The dissipated power of the plate is given by

$$P_{p,dis} = \omega \eta_p U_{max} = \omega \eta_p \left[\tilde{\mathbf{q}}^H \mathbf{K}_p \tilde{\mathbf{q}} \right] / 2 \tag{4.46}$$

where ω is the frequency, η_p is the structural loss factor of the plate, U_{max} is the maximum strain energy of the plate and $\mathbf{K}_p$ is the stiffness matrix represented in section 4.2. The dissipated power of the beams can be found similarly.

Thus it is expected that the power balance holds and corresponding the power balance equation is

$$P_{total} = P_{p,dis} + P_{b,dis} \tag{4.47}$$

where $P_{b,dis}$ is the total dissipated power in the four beams and P_{total} is the total input power. The numerical result is shown in Figure 9. This shows good agreement and the maximum difference between two powers is less than 0.001%.

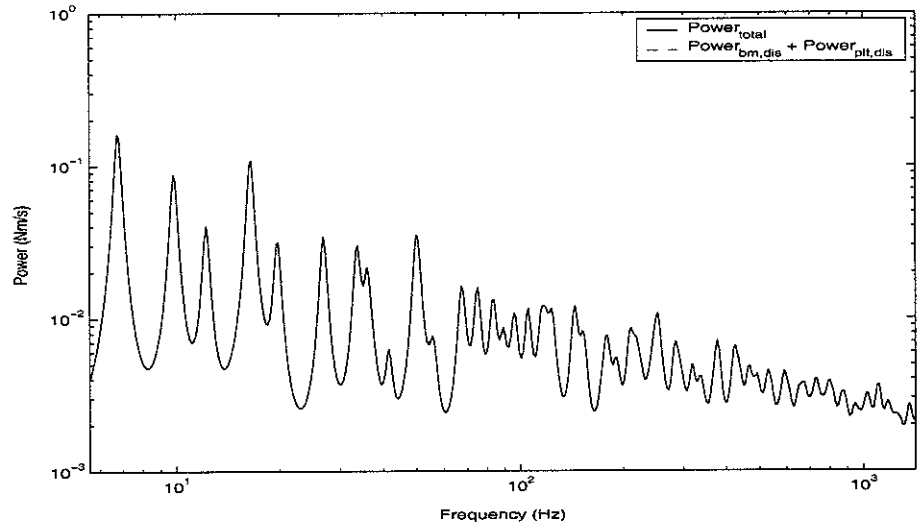

Figure 9. The power balance of the coupled structure consisting of four beams and a plate as in Figure 1 using a modal solution.

Although the modal method requires significant computational time and resources, it produces excellent responses such as mobilities. These results and the powers obtained in this section are used in the following section to compare with further development of the wave method.

5. ANALYSIS OF COUPLED SYSTEM USING A WAVE APPROACH

5.1 Wave approach

In the previous work [1, 2, 6], it was shown that a wave approach can conveniently be used for the analysis of a simple coupled structure such as a beam and a plate under certain assumptions. The most important restriction is that the wavenumber of the plate should be at least twice as large as that of the beam.

The wave method has also been applied to a more complicated system, where a box structure was investigated using the concept of the wave approach, although the spine structure was modelled using the FEM [7].

In the present report, the framed structure consisting of four beams and a rectangular plate is investigated. The beams possessing the long wavelength wave are modelled by the wave method instead of the FEM. In the previous section the framed structure shown in Figure 1 was analysed using the modal method, where the beam is assumed to be infinitely stiff so that the edges of the plate are in sliding. This same boundary condition is assumed in using the wave method to allow direct comparison. For such boundary conditions, the approximate wave impedance of the plate is [2]

$$\tilde{Z}'_p \approx \frac{\tilde{D}_p 2\tilde{k}_p^3}{\omega}\left(\frac{1-\tilde{\beta}_y\tilde{r}}{(1+\tilde{\beta}_y\tilde{r})-i(1-\tilde{\beta}_y\tilde{r})}\right) \tag{5.1}$$

where $\tilde{D}_p$ is the bending stiffness of the plate, $\tilde{k}_p$ is the plate free wavenumber, $\tilde{\beta}_y = e^{-i\tilde{k}_y 2L_y}$ is the propagating wave attenuation coefficient of the plate and $\tilde{r}$ is the complex reflection coefficient at the opposite edge of the plate at $y = L_y$, which is $\tilde{r} = 1$ for a sliding condition.

It should be noted that the terminology *width* in the wave method is always used to mean the dimension in the direction normal to the beam axis and the *opposite edge* means the plate edge parallel to the attached beam. Thus, L_y in equation (5.1) is the width of the finite plate between the beam axis lying at $y = 0$ and the opposite edge lying at $y = L_y$.

If the plate is infinitely wide so that $L_y = \infty$, then the approximate impedance of the plate is simply

$$\tilde{Z}'_p \approx \frac{\tilde{D}_p\tilde{k}_p^3}{\omega}(1+i) = \frac{m''_p\omega}{\tilde{k}_p}(1+i). \tag{5.2}$$

where m''_p is the mass per unit area of the plate.

Then the general dispersion equation for the built-up structure is given by

$$\tilde{D}_b \tilde{k}_x^4 = m_b' \omega^2 - i\omega \tilde{Z}_p' \tag{5.3}$$

where $\tilde{D}_b$ is the bending stiffness, m_b' is the mass per unit length of the beam and $\tilde{k}_x$ is the travelling wavenumber of the coupled beam/plate system in the direction of the beam. Note that as equation (5.1) includes the plate trace wavenumber $\tilde{k}_y$, an iterative method is required to find the coupled beam wavenumber $\tilde{k}_x$ in solving equations (5.3) and (5.1). However, some poles hardly converge with simple iteration and Muller's method was introduced to get a better result [2]. Once the coupled beam wavenumber is found and assuming the nearfield wavenumber is the same as the travelling wavenumber, the motion of the finite beam possessing the coupled wavenumber can be represented by

$$\tilde{w}_b(x) = \tilde{A}e^{-i\tilde{k}_x x} + \tilde{B}e^{-\tilde{k}_x x} + \tilde{C}e^{i\tilde{k}_x x} + \tilde{D}e^{\tilde{k}_x x} \tag{5.4}$$

where $\tilde{A}$ and $\tilde{C}$ are the amplitudes of travelling waves, $\tilde{B}$ and $\tilde{D}$ are the amplitudes of the nearfield waves.

5.2 Coupled structure consisting of four beams: application of the wave method

If it can be assumed that the power from the excited beam is not transferred to the other beams through the plate, the framed structure consisting of four beams and the rectangular plate can be represented by the system consisting of the four beams having the coupled wavenumber due to the plate impedance. Then such a system can be modelled simply using the wave method. The structure physically satisfying the above assumption is realised in Figure 10. In the figure, the *width* of the plates attached to beams 1 and 3 is L_y and for the plates attached to beams 2 and 4 the width is L_x.

As sliding edges are assumed in the framed structure in Figure 1, the same sliding boundary conditions at the opposite edges are used for the structure shown in Figure 10. This may result in different responses compared with those of the framed structure, as in fact the opposite edges should be attached to other beams. However, if the assumption explained above holds it is expected that their influence will reduce and although affecting the individual frequency behaviour this approach might still be useful for the mean response calculation.

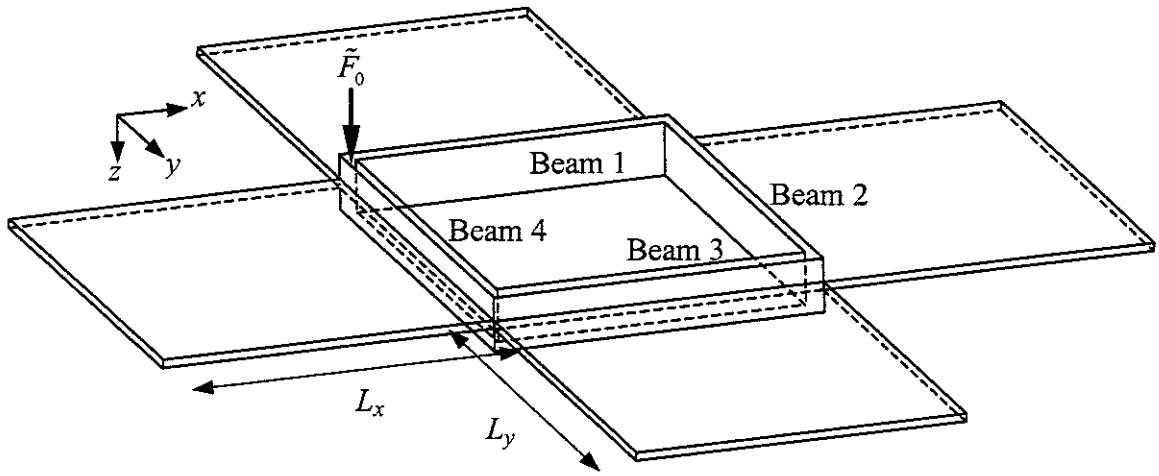

Figure 10. Configuration of the coupled structure for the use of the wave method.

The coupled structure can be modelled in terms of four beams having coupled wavenumber due to the plate impedance. The external force is applied at the corner of beam 1 and beam 4. Note that the coupled beam wavenumber to be used in modelling is based on the assumption that the opposite edges of the plates shown in Figure 10 are sliding. Thus, equation (5.1) is used in equation (5.3). Also, it is assumed that beams 1 and 3 are identical with the same (coupled) wavenumber $\tilde{k}_x$ and that beams 2 and 4 are identical with wavenumber $\tilde{k}_y$.

The method for obtaining the wave model is similar to that given in Appendix B. This describes a frame of four beams in which no plate is attached to the beams. Thus the beams possess the free beam wavenumber, $\tilde{k}_b$. The boundary conditions of the wave model consisting of four beams are also explained and these are the same as those used in the modal model. In order to model the structure shown in Figure 10, only the coupled wavenumber obtained from equation (5.3) needs to be substituted for the uncoupled beam wavenumber in the method of Appendix B.

5.3 Numerical results

5.3.1 Comparison with the modal method

As explained in the previous section, the wave approach is an approximate method and it is necessary to compare its results with other known methods. In section 4, the modal method and its numerical examples are shown for the framed structure and this gives good results. Thus the results based on the wave method are compared here with those of the modal

method. The highest modal order used in the modal method is 40 ($M = N = 40$, see section 4.3.2)

The first step in the wave analysis is to determine the wavenumbers of the corresponding subsystems of the coupled structure. Firstly the coupled beam wavenumbers k_x, k_y and the corresponding uncoupled wavenumbers are shown in Figure 11 (the wavenumbers for the uncoupled structures were already shown in Figure 2). It can be seen that, although the wavenumbers k_x and k_y follow the same asymptotic line, corresponding to a beam coupled to a semi-infinite plate, their peaks and troughs are different as the plate widths are different.

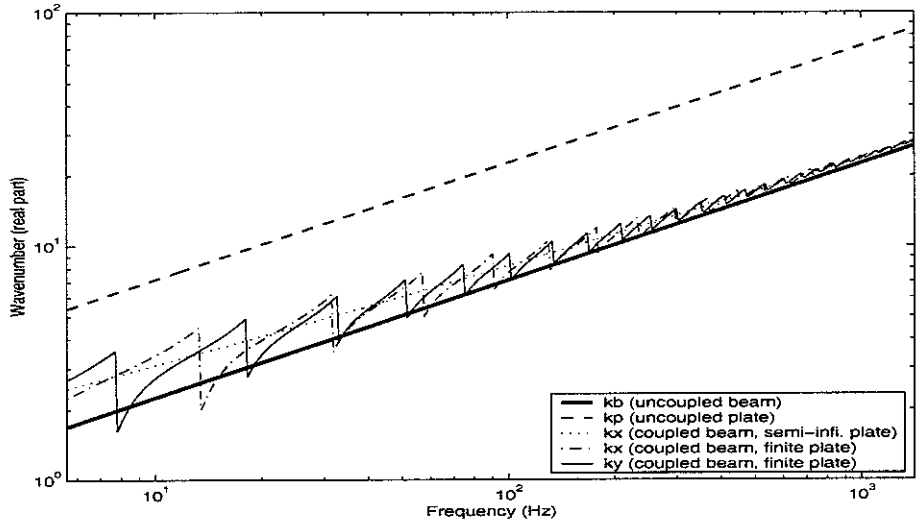

Figure 11. The coupled beam wavenumber k_x, k_y and the related wavenumbers.

It is interesting to compare the point mobilities of the two structures of Figures 10 and B.1 so the effect of the plate can be understood. They are compared in Figure 12, in which the result of the structure from Appendix B is the same as given in Figure B.2. It can be seen that there are many more resonance peaks when the plate is attached, due to the coupling with plate modes. However, one can also see that (i) the average vibrational level significantly decreases (ii) the height of the peaks and troughs is reduced. This is likely to be because the plate behaves like a mass and damping attached to the beam [1].

An asymptotic representation for the point mobility shown in Figure 12 may be useful to understand the effect of the plate. The asymptotic line of the point mobility of the framed structure can be obtained by making two adjacent beams semi-infinite in the structures shown in Figures 10 and B.1; the other two beams are in fact removed. Thus, for example beams 1

and 4 remain in Figure B.1 if an external force is applied the joint of those beams. The point mobility of such a system consisting of two semi-infinite beams at right angles can be found similarly as explained in Appendix B except that amplitudes $\tilde{C}$ and $\tilde{D}$ of the reflected waves in equation (B.1) should be zero. The sliding condition of the joint is not changed. The relevant equation of the point mobility is given by

$$\tilde{Y}_{x=0} = \frac{i\omega\tilde{w}(x=0)}{\tilde{F}_0} = \frac{(1-i)\omega}{4\tilde{D}_b\tilde{k}_b^3} \tag{5.5}$$

where $\tilde{k}_b$ is the beam wavenumber when the system is not coupled to plate. The effect of the plate coupled to the beam can be realised by replacing $\tilde{k}_b$ by the coupled beam wavenumber $\tilde{k}_x$ which is obtained in equations (5.2) and (5.3).

The asymptotic lines obtained by equation (5.5) are also represented in Figure 12. It can be seen that the coupled plate reduces the response level because of the added mass effect. This effect however decreases with increasing frequency as the effective mass due to the plate reduces [1].

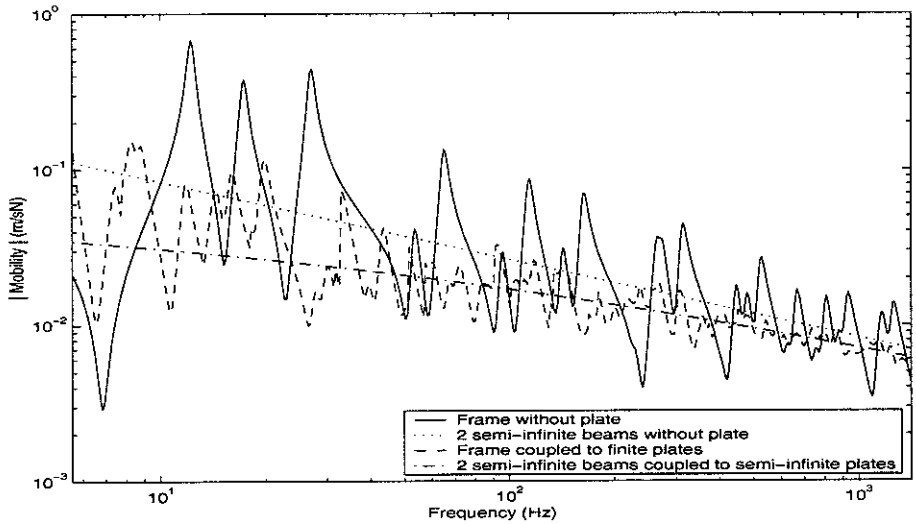

Figure 12. Point mobility comparison of the plate-coupled structure as in Figure 10 and the structure consisting of only four beams as in Figure B.1 (based on the wave method, excitation at $x = 0$).

The point mobility of the coupled system is compared with that predicted by the modal method in Figure 13. It can be seen that the results are in good agreement at high frequencies, although the lower natural frequencies show differences between the two methods. This will be discussed later.

It is also interesting to compare these point mobilities with that obtained when semi-infinite plates are assumed. The semi-infinite plate is realised by letting the *width* of the plates shown in Figure 10 be infinite and the corresponding wavenumber can be found using equation (5.2) instead of equation (5.1) in equation (5.3). This wavenumber is shown in Figure 11. One can see that the point mobilities oscillate around the line obtained due to the semi-infinite plate. It seems that most of the peaks may occur due to the oscillating finite plate. The damping added to the beams increases when the semi-infinite plate is introduced, resulting in a behaviour of the coupled structure similar to a heavily damped beam. It is known that the attached plate with a short wavelength behaves like a mass and damping on a beam possessing a long wavelength, such an arrangement being is called a fuzzy structure [14, 15]. Thus fuzzy theory is applicable to the present framed structure consisting of four beams and a rectangular plate as an approximate simplification.

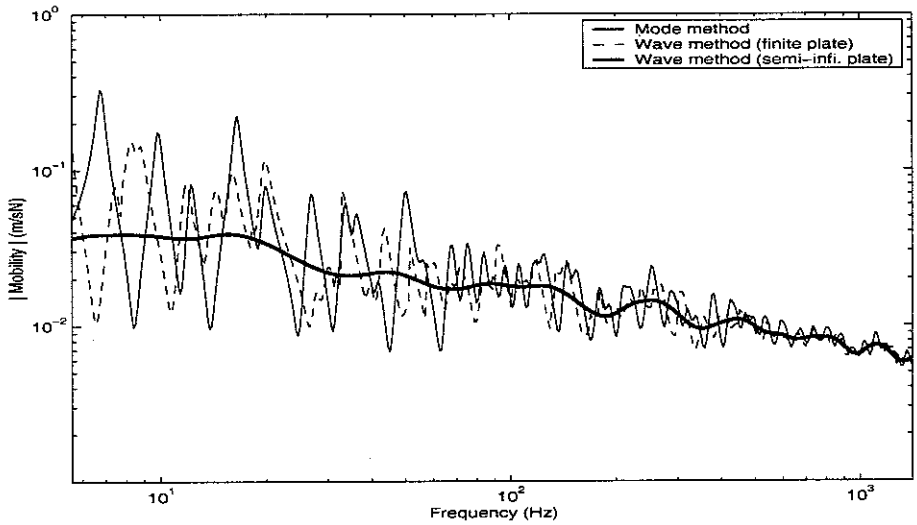

Figure 13. Point mobilities of the coupled structure as in Figure 10 based on the wave method and the modal method (excitation at $x = 0$).

The power transferred is compared for the two methods, where the corresponding equations based on the wave method are explained in [2]. Firstly, the power balance is investigated separately for both methods with the wave method result shown in Figure 14 (the result for the modal method was shown in Figure 9), where the power input and the total power (= power transferred to the plate + power dissipated in the beams) are compared. They show good agreement. The maximum error is 1.4%, which occurs due to the numerical integration used.

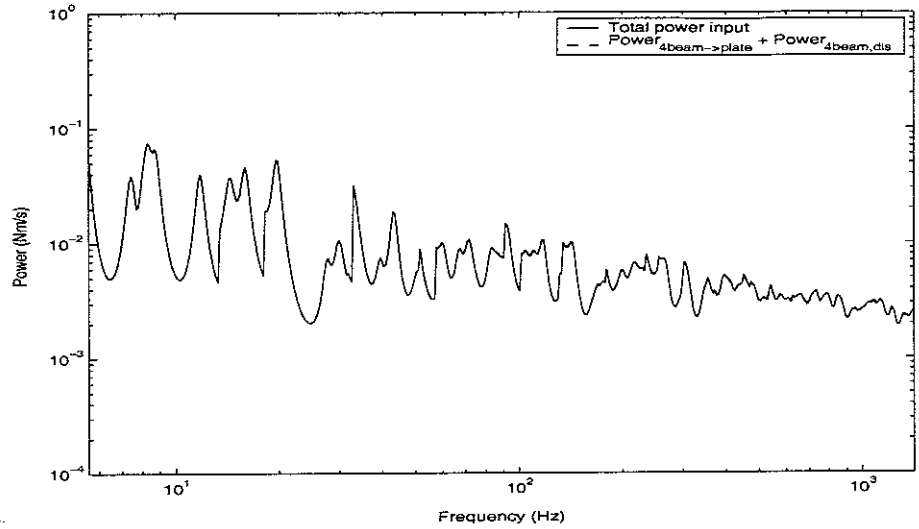

Figure 14. Power balance for the coupled structure as in Figure 10 using the wave method (point force is applied at $x = 0$ of beam 1 and finite plate is assumed).

The power transferred from the beams to the plate is next investigated, which will verify the assumption with respect to the power transfer explained in section 5.2. The power transferred from all the beams to the plate based on the wave method and the modal method are compared in Figure 15, where in fact for the modal method the dissipated power in the plate is given instead of the transferred power to reduce the calculation time. Similar to the point mobilities they show quite good agreement particularly at high frequencies.

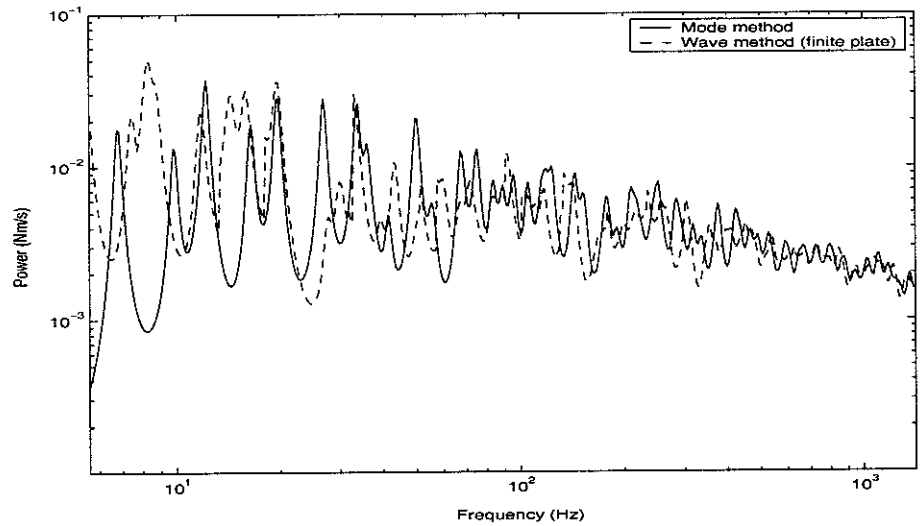

Figure 15. Power transfer from four beams to the coupled plate (point force is applied at $x = 0$ of beam 1 and finite width plates are assumed attached to the beams).

Since the exact location of resonance peaks is often of less interest than a frequency band average result, Figure 16 shows the results of Figure 15 converted into a 1/3 octave band form. The average values of the two methods agree, especially at high frequencies. The differences below about 60 Hz may occur because of differences in global modes between the structure shown in Figure 10, assumed for the wave method, and the framed structure used in the modal method (Figure 1). Thus the assumptions for the wave method do not appear to be appropriate for calculating the low frequency response and subsequent coupling power.

The average values are also compared with the result where attached semi-infinite plates are considered. Very good agreement can be observed at high frequencies.

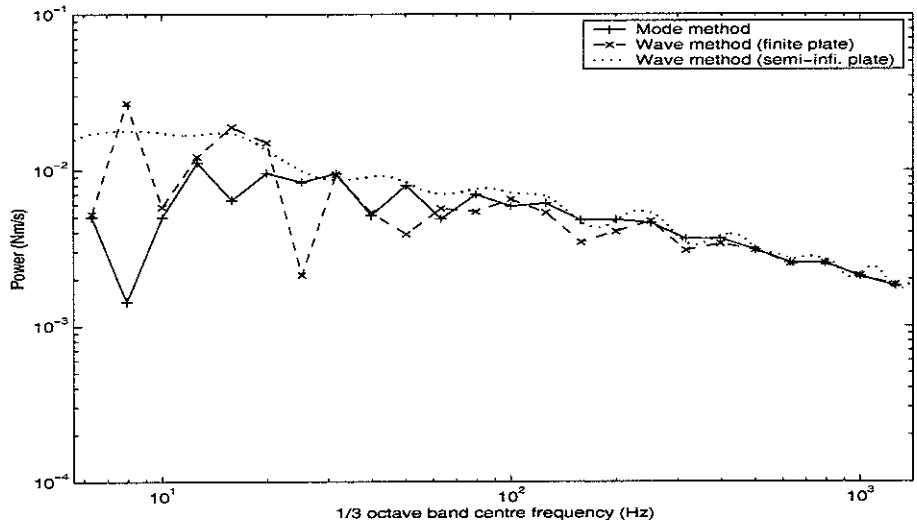

Figure 16. Power transfer from four beams to the plate in 1/3 octave bands (point force is applied at $x = 0$ of beam 1).

The results shown in Figure 16 imply that the average power transfer is hardly influenced by changes in the plate width. This is verified here by simply changing the plate width. The width of the plates attached to beams 1 and 3 is changed to $2L_y$ and for the plates attached to beams 2 and 4 the width is changed to $2L_x$ (see Figure 10). Note that the coupled wavenumbers are also changed. The results are shown in Figure 17. As expected, they show close agreement except at low frequencies, even though the width of all plates is changed. Small differences may occur because the plate is equivalent to being more heavily damped, as its width increases.

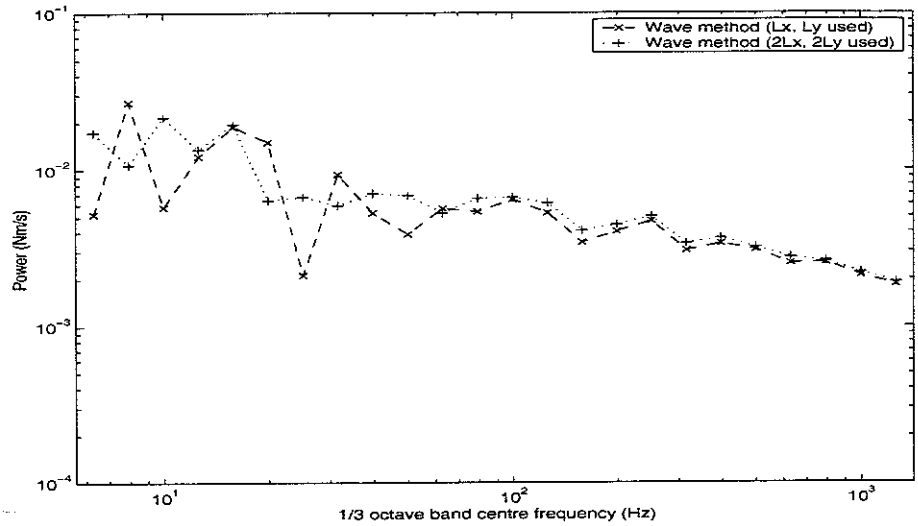

Figure 17. Comparison of power transfer when the plate width is changed in 1/3 octave bands (point force is applied at $x = 0$ of beam 1).

The total power input to the system based on the modal method and the wave method are compared in Figure 18 using the 1/3 octave band average. Comparing Figure 16 and Figure 18, one can observe similar tendencies in the difference between two methods. At least above about 60 Hz it seems that the hypothesis that the minimal power from the excited beam is transferred through the plate to the other beams is a reasonable assumption.

The hypothesis that the flexible plate transfers little energy between stiffer beams was already verified in a previous report [13] for a two-beam-plate coupled structure, in which the power transferred from the excited beam to the plate is around a factor of 10 greater than the power transferred from the plate to the opposite parallel beam. Thus most of the power is dissipated in the plate. It may be said that a similar phenomenon occurs for the system consisting of the two adjacent beams coupled to the plate. Consequently it can be said that most of the radiated power is absorbed in the plate and little is transferred to the connected beam through the plate.

This hypothesis can also be confirmed by comparing the power ratios between the two methods. If the ratios of the power transferred to the power input are similar for the modal method and the wave method, then this confirms the hypothesis. That is, the difference of the power transferred between the two methods shown in Figure 16 occurs not because the hypothesis is wrong but because of differences in the input power. However, if the ratios between the two methods are different, then it can be said that the hypothesis is wrong and the wave model is not acceptable.

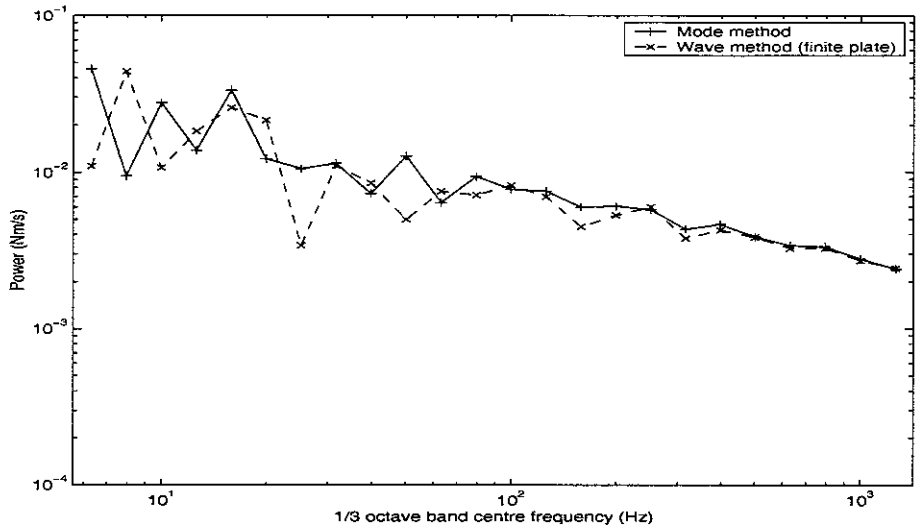

Figure 18. Comparison of input powers based on the modal method and the wave method in 1/3 octave bands (point force is applied at $x = 0$ of beam 1).

The power transfer from the four beams to the plate normalised to the power input for two methods are compared in Figure 19. It can be seen that the ratios based on the wave method and the modal method are in good agreement above about 60 Hz. This means that the fully framed structure as in Figure 1, can conveniently be analysed for power transfer estimates using the wave method. The assumption that the power is not transferred to the other beams through the plate is acceptable except at very low frequencies. In Figure 19 it can be seen that the difference is large at low frequencies. This shows that the wave model is not appropriate to represent the motion of the framed structure at these frequencies.

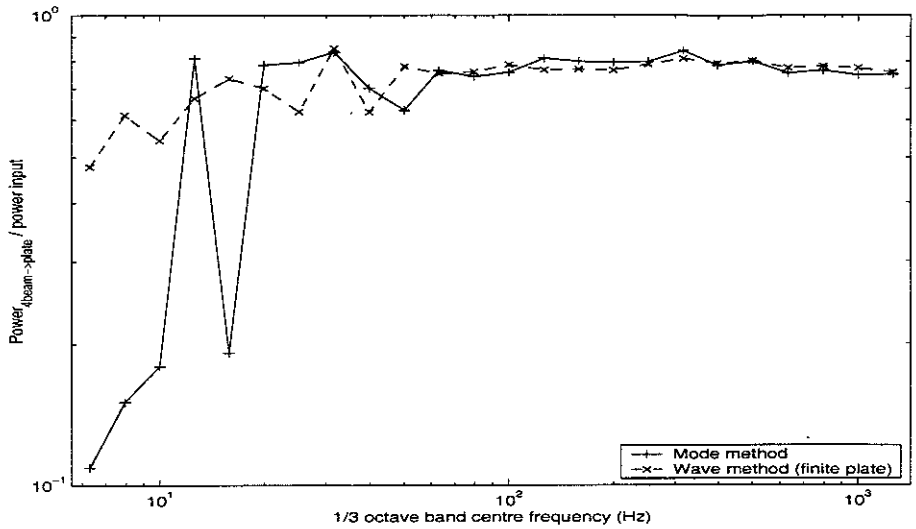

Figure 19. Comparison of power ratio (of power transfer from the four beams to the plate to the power input) based on the modal method and the wave method in 1/3 octave band average (point force is applied at $x = 0$ of beam 1).

5.3.2 Confidence interval for the power transfer

Although good qualitative agreement has been found between the two methods, as seen in Figure 15, the magnitude of the fluctuations relative to the average should also be considered. One possible way is to compare the confidence interval of the response so that the distribution of the power in a certain frequency band can be indicated. For this, overlapping octave bands are used at 1/3 octave band intervals.

The average value of the power is obtained for each octave band, $\overline{P}_{octave}$. Then the power at each frequency is normalised by the octave band average. The normalised power is calculated in dB as follows.

$$P_{dB} = 10\log_{10}\left(P/\overline{P}_{octave}\right) \tag{5.6}$$

where $P = P(\omega)$ is the power in a narrow band.

The 68% confidence interval of the normalised power P_{dB} is obtained explicitly for both the results based on the modal method and the wave method. The results are shown in Figure 20. It can be seen that the confidence interval follows the narrow band power very well, although it is not symmetrical with respect to the mean.

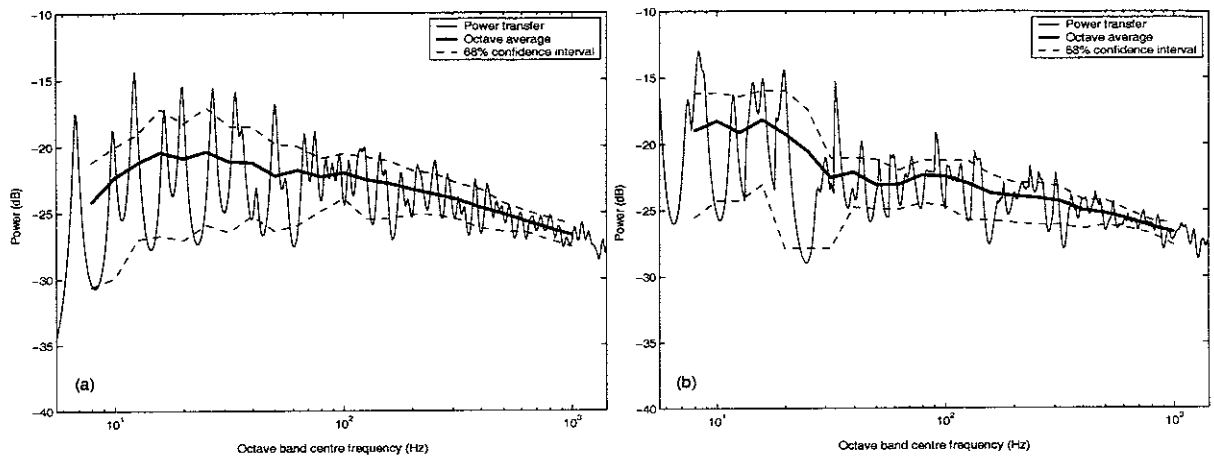

Figure 20. Octave band average and 68% confidence interval of the power transfer; (a) modal method (b) wave method (point force is applied at $x = 0$ of beam 1).

The confidence interval and the octave average shown in Figure 20 (a) and (b) are compared simultaneously in Figure 21. Comparing the confidence intervals one can see that they show good agreement at most frequencies especially above about 80 Hz. The difference in the level between the two methods occurs mainly because of the difference in the octave band average value.

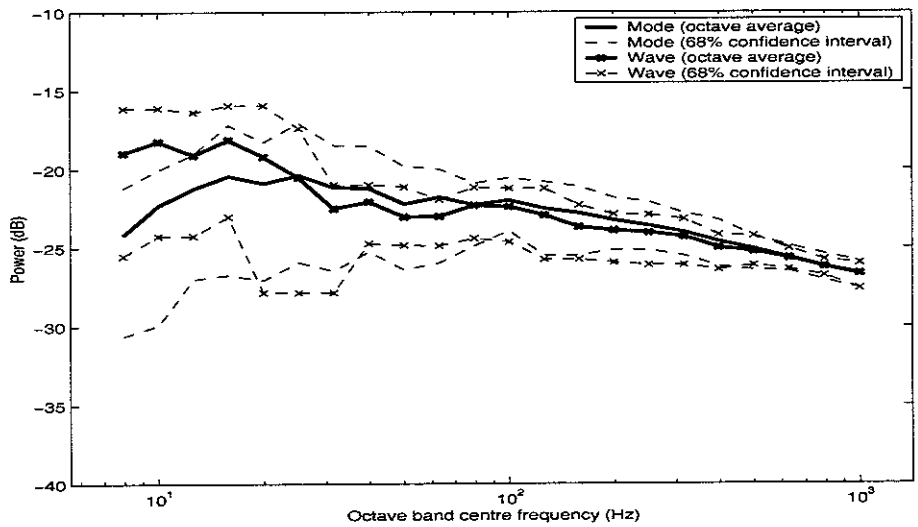

Figure 21. Octave band averages and 68 % confidence intervals of the power transfer based on the modal method and the wave method.

5.3.3 Discussion

The numerical results shown above indicate that the wave method is useful to obtain the response at mid and high frequencies. For example, the power transfer averaged in 1/3 octave bands is almost the same as that obtained using the modal method above about 60 Hz. To interpret this value of frequency, it may be noted that the stiff four-beam structure has only 5 resonant frequencies below 60 Hz (see Figure B.2) and the plate has less than 25 modes below 60 Hz. Thus in this low frequency region, the wave method is no longer appropriate as a coupling technique of the spine and the receiver structure. As the ratio between the plate and beam wavenumbers increases this low frequency limit to the method can be expected to reduce.

An important concern in practical applications is related to computer resources and calculation time. Here, one example of the calculation time comparison for the framed structure is shown in Table 3. Although the wave method can predict only approximate responses, one can see that it is very advantageous as it requires far less computer resources and time.

For reference, the computational time of the FEM is also given. In comparison of the modal method and the FE, it should be noted that the number of modes obtained by the FE for the forced response is 686, which is much less than that used in the modal method. Reducing the number of modes in the modal method results in much less computational time. For example, for the present case if 686 modes are considered in the modal method, the computational time significantly decreases to 40 minutes. In addition, compiled FE code is used in calculation whereas the modal method is solved by uncompiled Matlab code.

Table 3. Comparison of computational time (an Intel Pentium 4 computer (CPU 1500 MHz) is used in calculation).

	Computation time (min.)	Frequency range of calculation (Hz)	Comments
Modal method	360	5.6 - 1412	$M = N = 40$
Wave method	0.1	5.6 - 1412	-
FEM	12	0 - 2200	686 modes used

6. CONCLUSIONS

In the present report, a fully framed structure consisting of four beams and a rectangular plate was studied. Both ends of each beam and all the plate edges are assumed to be sliding. Using the modal method, the vibrational response of the framed structure was obtained. Then the wave method was applied to the same structure to obtain an approximate response. The results of the two methods were compared and useful observations and comments given.

The modal method and the Lagrangian formulation were used to produce an analytical model of the framed structure. The corresponding generalised mass and stiffness matrices for the coupled structure were found. Also, the procedure for derivation of the equations was presented. As the number of modes in the modal approach is an important factor for obtaining an accurate response, the dependency of the response on the number of modes included in the calculation was investigated. Then, the maximum mode numbers chosen were used for the modal model, which is considered to give an accurate response for the comparison with the wave model.

Although the modal method gives an accurate result, it is time-consuming and requires large computer resources as the frequency range increases. In addition, the detailed response such as exact natural frequencies is not of concern in the present study which deals with the mid and high frequencies. Thus an approximate method seems appropriate and the wave method was considered.

The analytical model based on the wave method for the dynamic response of the framed structure was presented. The statistical responses such as an octave average and a confidence interval of the power were obtained as well as the narrow band response. In comparison with the modal method it has been shown that the analytical wave model can conveniently be used for the estimation of the vibrational response in the mid and high frequency regions. In addition, it is shown that the width of the plate is not very critical in obtaining the average power transfer in a certain wide frequency band.

To apply the wave method it is necessary that the wavenumber of the free plate should be at least twice as large as that of any of the beams.

In the wave model consisting of four beams it is assumed that minimal power from the excited beam to the plate is subsequently transferred to the other beams. For the actual coupled structure considered, it was shown that this assumption is reasonable and holds.

The experimental validation for the framed structure which is shown in the present report is presently being examined. Principally, dynamic responses are being measured and the power relationship will be investigated in the test and will be compared with the results shown in this report.

REFERENCES

1. J. W. Yoo, N. S. Ferguson and D. J. Thompson 2002 *ISVR Memorandom No*: **888.** Structural analysis of a combined beam and plate structure using a wave approach.

2. J. W. Yoo, D. J. Thompson and N. S. Ferguson 2003 *ISVR Memorandom No*: **905.** Structural analysis of a symmetric structure consisting of two beams and a plate based on a wave approach.

3. J. W. Yoo, D. J. Thompson and N. S. Ferguson 2004 *ISVR Memorandom No*: **931.** Investigation of the coupling of a structure consisting of a beam and a plate in terms of statistical energy analysis.

4. H. Takabatake and Y. Nagareda 1999 *Computers and Structures* **70.** 129-139. A simplified analysis of elastic plates with edge beams.

5. J. Yang and A. Gupta 2002 *Journal of Sound and Vibration* **253.** 373-388. Ritz vector approach for static and dynamic analysis of plates with edge beams.

6. R. M. Grice and R. J. Pinnington 1999 *Journal of Sound and Vibration* **230,** 825-849. A method for the vibrational analysis of built-up structures, part 1: Introduction and analytical analysis of the plate-stiffened beam.

7. R. M. Grice and R. J. Pinnington 2002 *Journal of Sound and Vibration* **249.** 499-527. Analysis of the flexural vibration of a thin-plate box using a combination of finite element analysis and analytical impedance

8. L. Meirovich 1986 *Elements of vibration analysis.* New York: McGraw-Hill; 2nd edition.

9. R. Szilard 1974 *Theory and analysis of plates: classical and numerical methods.* New Jersey: Prentice-Hall.

10. R. E. D. Bishop and D. C. *Johnson 1960 Mechanics of vibration.* London: The Cambridge University press.

11. W. L. Thomson 1972 *Theory of vibration with applications.* New Jersey: Prentice-Hall.

12. S. S. Rao 1995 *Mechanical vibrations.* Addison-Wesley Publishing Company; third edition

13. J. W. Yoo, D. J. Thompson and N. S. Ferguson 2003 *ISVR Memorandom No*: **927.** A Fourier technique for the analysis of beam-plate coupled structure.

14. M. Strasberg and D. Feit 1996 *Journal of the Acoustical Society of America* **99,** 335-344. Vibration damping of large structures induced by attached small resonant structures.

15. C. Soize 1993 *Journal of the Acoustical Society of America* **94**, 849-865. A model and numerical method in the medium frequency range for vibroacoustic predictions using the theory of structural fuzzy.
16. D. J. Ewins 2000 *Modal testing: theory, practice and application*. Baldock: Research studies press; second edition

APPENDIX A. NOMENCLATURE

A	wave amplitude (m)
B	wave amplitude (m)
C	wave amplitude (m)
D	wave amplitude (m); beam stiffness (Nm^2); plate stiffness (Nm);
E	Young's modulus of elasticity (N/m^2); energy
F	force
$\mathbf{K}$	stiffness matrix
K	generalised stiffness; function stiffness
L	Lagrangian
L_x	length of a beam (m)
L_y	width of a plate (m)
$\mathbf{M}$	mass matrix
M	generalised mass; function mass; maximum mode number
N	maximum mode number; number of data
P	power (Nm/s)
T	kinetic energy
U	potential (strain) energy
Z'_p	line impedance of a plate
c	confidence interval
e	frequency and space-averaged error
f	frequency (Hz); force function
h	height of a beam
i	$\sqrt{-1}$
k_b	uncoupled beam wavenumber
k_p	uncoupled free wavenumber in a plate
k_x	coupled travelling trace wavenumber in x direction
k_y	coupled travelling trace wavenumber in y direction
m	mode number
m'_b	mass per unit length of a beam (kg/m)

m_p''	mass per unit area of a plate (kg/m^2)
n	mode number; Fourier component number
$\mathbf{q}$	matrix containing q
q	generalised coordinate
r	mode number
$\tilde{r}$	complex reflection coefficient
s	mode number
t	thickness (m)
w	displacement (m)
x, y, z	co-ordinates
$\mathbf{\Psi}$	matrix containing mode shape function ψ
$\tilde{\beta}$	wave attenuation coefficient
γ	non-dimensional wavenumber ($= k_x / k_b$)
δ	constant; Krönecker delta
η	structural loss factor (-)
ν	Poisson's ratio
ρ	density (kg/m^3)
σ	standard deviation
ϕ	mode shape function
ψ	mode shape function
μ	mean
ω	radian frequency (rad/s)

APPENDIX B. WAVE MODEL OF A FRAME CONSISTING OF FOUR BEAMS

B.1 Equations of motion

A rectangular frame structure consisting of four identical cross-section beams is considered, as shown in Figure B.1. This is solved using a wave approach. Each beam carries free waves with wavenumber $\tilde{k}_b^4 = m_b'/\tilde{D}_b\,\omega^2$ in harmonic motion at frequency ω. An external force is applied at the corner of beams 1 and 4. Each beam is assumed infinitely stiff to torsion. Damping is induced through a complex bending stiffness $\tilde{D}_b$.

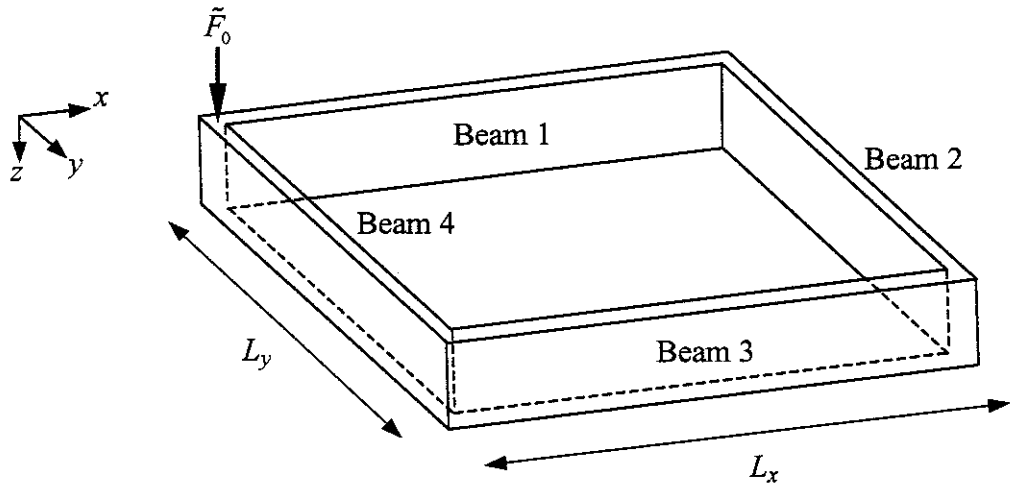

Figure B.1. The wave model consisting of four beams.

The boundary conditions for the four-beam structure as in Figure B.1 are:

(i) Continuity equation; equal displacement at corners

(ii) No rotation at the ends of the beams

(iii) Force equilibrium at the corners

The displacement of each beam can be given by an equation of the following form, shown for example for beam 1

$$\tilde{w}_1(x) = \tilde{A}_1 e^{-i\tilde{k}_b x} + \tilde{B}_1 e^{-\tilde{k}_b x} + \tilde{C}_1 e^{i\tilde{k}_b x} + \tilde{D}_1 e^{\tilde{k}_b x} \qquad \text{(B.1)}$$

where the subscripts of the equation mean they belong to beam 1. Then, from the first boundary condition, the same displacement at the corner of beam 1 and beam 2 gives

$$\tilde{w}_1\big|_{x=L_x} = \tilde{w}_2\big|_{y=0} \qquad \text{(B.2a)}$$

(B.2b)

$$\tilde{A}_1 e^{-i\tilde{k}_b L_x} + \tilde{B}_1 e^{-\tilde{k}_b L_x} + \tilde{C}_1 e^{i\tilde{k}_b L_x} + \tilde{D}_1 e^{\tilde{k}_b L_x} - \tilde{A}_2 - \tilde{B}_2 - \tilde{C}_2 - \tilde{D}_2 = 0.$$

The same boundary condition for beam 2 and beam 3 gives

$$\tilde{w}_2\big|_{y=L_y} = \tilde{w}_3\big|_{x=L_x} \tag{B.3a}$$

$$\begin{aligned}&\tilde{A}_2 e^{-i\tilde{k}_b L_y} + \tilde{B}_2 e^{-\tilde{k}_b L_y} + \tilde{C}_2 e^{i\tilde{k}_b L_y} + \tilde{D}_2 e^{\tilde{k}_b L_y} \\ &-\tilde{A}_3 e^{-i\tilde{k}_b L_x} - \tilde{B}_3 e^{-\tilde{k}_b L_x} - \tilde{C}_3 e^{i\tilde{k}_b L_x} - \tilde{D}_3 e^{\tilde{k}_b L_x} = 0.\end{aligned} \tag{B.3b}$$

For beam 3 and beam 4,

$$\tilde{w}_4\big|_{y=L_y} = \tilde{w}_3\big|_{x=0} \tag{B.4a}$$

$$\tilde{A}_4 e^{-i\tilde{k}_b L_y} + \tilde{B}_4 e^{-\tilde{k}_b L_y} + \tilde{C}_4 e^{i\tilde{k}_b L_y} + \tilde{D}_4 e^{\tilde{k}_b L_y} - \tilde{A}_3 - \tilde{B}_3 - \tilde{C}_3 - \tilde{D}_3 = 0. \tag{B.4b}$$

For beam 1 and beam 4,

$$\tilde{w}_1\big|_{x=0} = \tilde{w}_4\big|_{y=0} \tag{B.5a}$$

$$\tilde{A}_1 + \tilde{B}_1 + \tilde{C}_1 + \tilde{D}_1 - \tilde{A}_4 - \tilde{B}_4 - \tilde{C}_4 - \tilde{D}_4 = 0. \tag{B.5b}$$

The condition of no rotation is applied to the ends of the beam, the relevant equation of which for beam 1 is

$$\frac{d\tilde{w}_1(x)}{dx} = -i\tilde{k}_b \tilde{A}_1 e^{-i\tilde{k}_b x} - \tilde{k}_b \tilde{B}_1 e^{-\tilde{k}_b x} + i\tilde{k}_b \tilde{C}_1 e^{i\tilde{k}_b x} + \tilde{k}_b \tilde{D}_1 e^{\tilde{k}_b x} = 0. \tag{B.6}$$

Thus, the two equations given by boundary condition (ii) for beam 1 are

$$\left.\frac{d\tilde{w}_1(x)}{dx}\right|_{x=0} = -i\tilde{k}_b \tilde{A}_1 - \tilde{k}_b \tilde{B}_1 + i\tilde{k}_b \tilde{C}_1 + \tilde{k}_b \tilde{D}_1 = 0 \tag{B.7}$$

and

$$\left.\frac{d\tilde{w}_1(x)}{dx}\right|_{x=L_x} = -i\tilde{k}_b \tilde{A}_1 e^{-i\tilde{k}_b L_x} - \tilde{k}_b \tilde{B}_1 e^{-\tilde{k}_b L_x} + i\tilde{k}_b \tilde{C}_1 e^{i\tilde{k}_b L_x} + \tilde{k}_b \tilde{D}_1 e^{\tilde{k}_b L_x} = 0. \tag{B.8}$$

For beam 2,

$$\left.\frac{d\tilde{w}_2(y)}{dy}\right|_{y=0} = -i\tilde{k}_b \tilde{A}_2 - \tilde{k}_b \tilde{B}_2 + i\tilde{k}_b \tilde{C}_2 + \tilde{k}_b \tilde{D}_2 = 0 \tag{B.9}$$

and

$$\left.\frac{d\tilde{w}_2(y)}{dy}\right|_{y=L_y} = -i\tilde{k}_b\tilde{A}_2 e^{-i\tilde{k}_b L_y} - \tilde{k}_b\tilde{B}_2 e^{-\tilde{k}_b L_y} + i\tilde{k}_b\tilde{C}_2 e^{i\tilde{k}_b L_y} + \tilde{k}_b\tilde{D}_2 e^{\tilde{k}_b L_y} = 0. \tag{B.10}$$

For beam 3,

$$\left.\frac{d\tilde{w}_3(x)}{dx}\right|_{x=0} = -i\tilde{k}_b\tilde{A}_3 - \tilde{k}_b\tilde{B}_3 + i\tilde{k}_b\tilde{C}_3 + \tilde{k}_b\tilde{D}_3 = 0 \tag{B.11}$$

and

$$\left.\frac{d\tilde{w}_3(x)}{dx}\right|_{x=L_x} = -i\tilde{k}_b\tilde{A}_3 e^{-i\tilde{k}_b L_x} - \tilde{k}_b\tilde{B}_3 e^{-\tilde{k}_b L_x} + i\tilde{k}_b\tilde{C}_3 e^{i\tilde{k}_b L_x} + \tilde{k}_b\tilde{D}_3 e^{\tilde{k}_b L_x} = 0. \tag{B.12}$$

For beam 4,

$$\left.\frac{d\tilde{w}_4(y)}{dy}\right|_{y=0} = -i\tilde{k}_b\tilde{A}_4 - \tilde{k}_b\tilde{B}_4 + i\tilde{k}_b\tilde{C}_4 + \tilde{k}_b\tilde{D}_4 = 0 \tag{B.13}$$

and

$$\left.\frac{d\tilde{w}_4(y)}{dy}\right|_{y=L_y} = -i\tilde{k}_b\tilde{A}_4 e^{-i\tilde{k}_b L_y} - \tilde{k}_b\tilde{B}_4 e^{-\tilde{k}_b L_y} + i\tilde{k}_b\tilde{C}_4 e^{i\tilde{k}_b L_y} + \tilde{k}_b\tilde{D}_4 e^{\tilde{k}_b L_y} = 0. \tag{B.14}$$

The shear force acting on beam 1 is given by

$$\tilde{F}_1 = -\tilde{D}_b\frac{d^3\tilde{w}_1(x)}{dx^3} = -\tilde{D}_b\left(i\tilde{k}_b^3\tilde{A}_1 e^{-i\tilde{k}_b x} - \tilde{k}_b^3\tilde{B}_1 e^{-\tilde{k}_b x} - i\tilde{k}_b^3\tilde{C}_1 e^{i\tilde{k}_b x} + \tilde{k}_b^3\tilde{D}_1 e^{\tilde{k}_b x}\right). \tag{B.15}$$

where $\tilde{D}_b$ is the bending stiffness of the beam.

As the force equilibrium holds at the corner where two beams join, the corresponding boundary equation can be found. For beam 1 and beam 2 the equation is

$$-\tilde{F}_1\big|_{x=L_x} + \tilde{F}_2\big|_{y=0} = 0 \tag{B.16a}$$

$$\left(i\tilde{k}_b^3\tilde{A}_1 e^{-i\tilde{k}_b L_x} - \tilde{k}_b^3\tilde{B}_1 e^{-\tilde{k}_b L_x} - i\tilde{k}_b^3\tilde{C}_1 e^{i\tilde{k}_b L_x} + \tilde{k}_b^3\tilde{D}_1 e^{\tilde{k}_b L_x}\right)$$
$$-\left(i\tilde{k}_b^3\tilde{A}_2 - \tilde{k}_b^3\tilde{B}_2 - i\tilde{k}_b^3\tilde{C}_2 + \tilde{k}_b^3\tilde{D}_2\right) = 0. \tag{B.16b}$$

For beams 2 and 3, it is

$$-\tilde{F}_2\big|_{y=L_y} - \tilde{F}_3\big|_{x=L_x} = 0 \tag{B.17a}$$

$$\left(i\tilde{k}_b^3\tilde{A}_2 e^{-i\tilde{k}_b L_y} - \tilde{k}_b^3\tilde{B}_2 e^{-\tilde{k}_b L_y} - i\tilde{k}_b^3\tilde{C}_2 e^{i\tilde{k}_b L_y} + \tilde{k}_b^3\tilde{D}_2 e^{\tilde{k}_b L_y}\right)$$
$$+\left(i\tilde{k}_b^3\tilde{A}_3 e^{-i\tilde{k}_b L_x} - \tilde{k}_b^3\tilde{B}_3 e^{-\tilde{k}_b L_x} - i\tilde{k}_b^3\tilde{C}_3 e^{i\tilde{k}_b L_x} + \tilde{k}_b^3\tilde{D}_3 e^{\tilde{k}_b L_x}\right) = 0. \tag{B.17b}$$

For beams 3 and 4,

$$-\tilde{F}_4\Big|_{y=L_y}+\tilde{F}_3\Big|_{x=0}=0 \tag{B.18a}$$

$$\left(i\tilde{k}_b^3\tilde{A}_4e^{-i\tilde{k}_bL_y}-\tilde{k}_b^3\tilde{B}_4e^{-\tilde{k}_bL_y}-i\tilde{k}_b^3\tilde{C}_4e^{i\tilde{k}_bL_y}+\tilde{k}_b^3\tilde{D}_4e^{\tilde{k}_bL_y}\right)$$
$$-\left(i\tilde{k}_b^3\tilde{A}_3-\tilde{k}_b^3\tilde{B}_3-i\tilde{k}_b^3\tilde{C}_3+\tilde{k}_b^3\tilde{D}_3\right)=0 \tag{B.18b}$$

For beams 4 and 1, the external force applied at the corner should be included in the equilibrium condition. Thus the corresponding equation is

$$\tilde{F}_1\Big|_{x=0}+\tilde{F}_4\Big|_{y=0}+\tilde{F}_0=0 \tag{B.19a}$$

$$-\tilde{D}_b\left(i\tilde{k}_b^3\tilde{A}_1-\tilde{k}_b^3\tilde{B}_1-i\tilde{k}_b^3\tilde{C}_1+\tilde{k}_b^3\tilde{D}_1\right)-\tilde{D}_b\left(i\tilde{k}_b^3\tilde{A}_4-\tilde{k}_b^3\tilde{B}_4-i\tilde{k}_b^3\tilde{C}_4+\tilde{k}_b^3\tilde{D}_4\right)+\tilde{F}_0=0$$

$$\left(i\tilde{k}_b^3\tilde{A}_1-\tilde{k}_b^3\tilde{B}_1-i\tilde{k}_b^3\tilde{C}_1+\tilde{k}_b^3\tilde{D}_1\right)+\left(i\tilde{k}_b^3\tilde{A}_4-\tilde{k}_b^3\tilde{B}_4-i\tilde{k}_b^3\tilde{C}_4+\tilde{k}_b^3\tilde{D}_4\right)=\tilde{F}_0/\tilde{D}_b \tag{B.19b}$$

Then, equations (B.2b) - (B.5b), (B.7) - (B.14) and (B.16b) - (B.19b) can be written into a matrix form.

$$\mathbf{Ku}=\mathbf{F} \tag{B.20}$$

where $\mathbf{K}$ is given by

$$\mathbf{K}=\begin{bmatrix}
e^{-i\tilde{k}_bL_x} & e^{-\tilde{k}_bL_x} & e^{i\tilde{k}_bL_x} & e^{\tilde{k}_bL_x} & -1 & -1 & -1 & -1 & 0 & 0 & 0 & 0 & 0 & 0 & 0 & 0\\
0 & 0 & 0 & 0 & e^{-i\tilde{k}_bL_y} & e^{-\tilde{k}_bL_y} & e^{i\tilde{k}_bL_y} & e^{\tilde{k}_bL_y} & -e^{-i\tilde{k}_bL_x} & -e^{-\tilde{k}_bL_x} & -e^{i\tilde{k}_bL_x} & -e^{\tilde{k}_bL_x} & 0 & 0 & 0 & 0\\
0 & 0 & 0 & 0 & 0 & 0 & 0 & 0 & -1 & -1 & -1 & -1 & e^{-i\tilde{k}_bL_y} & e^{-\tilde{k}_bL_y} & e^{i\tilde{k}_bL_y} & e^{\tilde{k}_bL_y}\\
1 & 1 & 1 & 1 & 0 & 0 & 0 & 0 & 0 & 0 & 0 & 0 & -1 & -1 & -1 & -1\\
-i\tilde{k}_b & -\tilde{k}_b & i\tilde{k}_b & \tilde{k}_b & 0 & 0 & 0 & 0 & 0 & 0 & 0 & 0 & 0 & 0 & 0 & 0\\
-i\tilde{k}_be^{-i\tilde{k}_bL_x} & -\tilde{k}_be^{-\tilde{k}_bL_x} & i\tilde{k}_be^{i\tilde{k}_bL_x} & \tilde{k}_be^{\tilde{k}_bL_x} & 0 & 0 & 0 & 0 & 0 & 0 & 0 & 0 & 0 & 0 & 0 & 0\\
0 & 0 & 0 & 0 & -i\tilde{k}_b & -\tilde{k}_b & i\tilde{k}_b & \tilde{k}_b & 0 & 0 & 0 & 0 & 0 & 0 & 0 & 0\\
0 & 0 & 0 & 0 & -i\tilde{k}_be^{-i\tilde{k}_bL_y} & -\tilde{k}_be^{-\tilde{k}_bL_y} & i\tilde{k}_be^{i\tilde{k}_bL_y} & \tilde{k}_be^{\tilde{k}_bL_y} & 0 & 0 & 0 & 0 & 0 & 0 & 0 & 0\\
0 & 0 & 0 & 0 & 0 & 0 & 0 & 0 & -i\tilde{k}_b & -\tilde{k}_b & i\tilde{k}_b & \tilde{k}_b & 0 & 0 & 0 & 0\\
0 & 0 & 0 & 0 & 0 & 0 & 0 & 0 & -i\tilde{k}_be^{-i\tilde{k}_bL_x} & -\tilde{k}_be^{-\tilde{k}_bL_x} & i\tilde{k}_be^{i\tilde{k}_bL_x} & \tilde{k}_be^{\tilde{k}_bL_x} & 0 & 0 & 0 & 0\\
0 & 0 & 0 & 0 & 0 & 0 & 0 & 0 & 0 & 0 & 0 & 0 & -i\tilde{k}_b & -\tilde{k}_b & i\tilde{k}_b & \tilde{k}_b\\
0 & 0 & 0 & 0 & 0 & 0 & 0 & 0 & 0 & 0 & 0 & 0 & -i\tilde{k}_be^{-i\tilde{k}_bL_y} & -\tilde{k}_be^{-\tilde{k}_bL_y} & i\tilde{k}_be^{i\tilde{k}_bL_y} & \tilde{k}_be^{\tilde{k}_bL_y}\\
i\tilde{k}_b^3e^{-i\tilde{k}_bL_x} & -\tilde{k}_b^3e^{-\tilde{k}_bL_x} & -i\tilde{k}_b^3e^{i\tilde{k}_bL_x} & \tilde{k}_b^3e^{\tilde{k}_bL_x} & -i\tilde{k}_b^3 & \tilde{k}_b^3 & i\tilde{k}_b^3 & -\tilde{k}_b^3 & 0 & 0 & 0 & 0 & 0 & 0 & 0 & 0\\
0 & 0 & 0 & 0 & i\tilde{k}_b^3e^{-i\tilde{k}_bL_y} & -\tilde{k}_b^3e^{-\tilde{k}_bL_y} & -i\tilde{k}_b^3e^{i\tilde{k}_bL_y} & \tilde{k}_b^3e^{\tilde{k}_bL_y} & i\tilde{k}_b^3e^{-i\tilde{k}_bL_x} & -\tilde{k}_b^3e^{-\tilde{k}_bL_x} & -i\tilde{k}_b^3e^{i\tilde{k}_bL_x} & \tilde{k}_b^3e^{\tilde{k}_bL_x} & 0 & 0 & 0 & 0\\
0 & 0 & 0 & 0 & 0 & 0 & 0 & 0 & -i\tilde{k}_b^3 & \tilde{k}_b^3 & i\tilde{k}_b^3 & -\tilde{k}_b^3 & i\tilde{k}_b^3e^{-i\tilde{k}_bL_y} & -\tilde{k}_b^3e^{-\tilde{k}_bL_y} & -i\tilde{k}_b^3e^{i\tilde{k}_bL_y} & \tilde{k}_b^3e^{\tilde{k}_bL_y}\\
i\tilde{k}_b^3 & -\tilde{k}_b^3 & -i\tilde{k}_b^3 & \tilde{k}_b^3 & 0 & 0 & 0 & 0 & 0 & 0 & 0 & 0 & i\tilde{k}_b^3 & -\tilde{k}_b^3 & -i\tilde{k}_b^3 & \tilde{k}_b^3
\end{bmatrix} \tag{B.21}$$

the force vector, $\mathbf{F}$ is

$$\mathbf{F}=\begin{bmatrix}0 & 0 & 0 & 0 & 0 & 0 & 0 & 0 & 0 & 0 & 0 & 0 & 0 & 0 & 0 & \tilde{F}_0/\tilde{D}_b\end{bmatrix}^T \tag{B.22}$$

and the displacement vector is

$$\mathbf{u} = \left[\tilde{A}_1 \quad \tilde{B}_1 \quad \tilde{C}_1 \quad \tilde{D}_1 \quad \tilde{A}_2 \quad \tilde{B}_2 \quad \tilde{C}_2 \quad \tilde{D}_2 \quad \tilde{A}_3 \quad \tilde{B}_3 \quad \tilde{C}_3 \quad \tilde{D}_3 \quad \tilde{A}_4 \quad \tilde{B}_4 \quad \tilde{C}_4 \quad \tilde{D}_4 \right]^T . \tag{B.23}$$

The displacement of any beam of the coupled structure shown in Figure B.1 can be found from

$$\mathbf{u} = \mathbf{K}^{-1}\mathbf{F} \tag{B.24}$$

allowing $w_i(x)$ to be found from equation (B.1).

B.2 Numerical results

As an example, the point mobility of the structure shown in Figure B.1 is given here in Figure B.2. The relevant dimensions of the structure are the same as written in Table 1 except that no plate is attached to the beams. The beam model used in the FEM is the same as explained in section 4.3.2. The result is compared with that of FE and they are not distinguishable (maximum error of 0.6%).

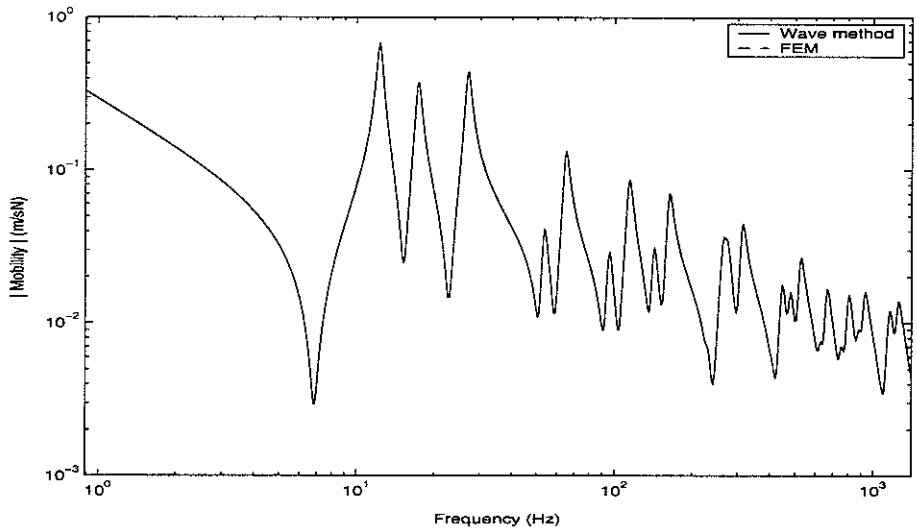

Figure B.2. Point mobility comparison between the wave model and the FE (excitation at $x = 0$ and $y = 0$).

In the present report, the rotational stiffness of a beam is assumed to be infinitely stiff. The effect of the torsional stiffness of the rectangular frame structure as in Figure B.1 is identified. In the FE model the torsional stiffness can simply be realised by releasing the rotational Degree Of Freedom (DOF) fixed to describe the infinite stiffness of torsion.

Consequently, the sliding boundary condition for the ends of the beam is no longer applied. The results are compared in Table B.1 and Figure B.3.

Table B.1 shows the Modal Assurance Criterion value (MAC, [16]), which shows the spatial correlation between the mode shapes obtained with and without the sliding. The table shows only the modes below 100 Hz of the system without sliding conditions, which are compared with the sliding - constrained modes. A MAC value equal to unity means that the two modes considered are identical. By allowing the torsional motion of the beams, the natural frequencies of the framed structure occur at lower frequencies than when restrained. For example, it can be seen that the sliding constraint mode at 26.9 Hz is similar to a mode for the system without the sliding constraints occurring at 10.4 Hz. The unconstrained system has three rigid body modes, whereas with the sliding constraints there is only one*. Constraining the beam rotation results in the modes corresponding to 12.2 and 17.3 Hz shown in Table B.1. These modes correspond to a half cosine motion on two opposite beams and rigid motion of the other two beams. Thus, they are rather closer to the rigid modes than other dynamic modes of the system without constraints. So, comparing the dynamic modes of the two systems, although the natural frequencies are significantly changed by the different boundary conditions, the mode shapes are not very different.

Table B.1. Modal Assurance Criterion between the mode shapes with sliding constraints and without sliding constraints (a zero corresponds to a MAC value of less than 1.0×10^{-3}).

		Modes without sliding constraints (Hz)								
		0	0	0	10.4	24.2	37.8	53.1	63.1	96.9
Modes with sliding constraints (Hz)	0	**0.61**	0.32	0.07	0	0	0	0	0	0
	12.2	0.38	**0.48**	0.13	0	0	0	0	0	0
	17.3	0	0.19	**0.80**	0	0	0	0	0	0
	26.9	0	0	0	**0.99**	0	0	0	0	0
	53.3	0	0	0	0	**0.96**	0	0	0.01	0
	64.8	0	0	0	0	0	**0.97**	0	0	0
	95.0	0	0	0	0	0	0	**0.96**	0	0
	113	0	0	0	0	0.01	0	0	**0.95**	0
	142	0	0	0	0	0	0	0	0	**0.95**

* Here, translational rigid modes in x and y directions and a rotational rigid mode with respect to z direction are not included as the FE model is made for comparison with the wave model.

The point mobilities are compared in Figure B.3. It can also be seen that allowing the torsional motion of the beam increases the response level as the framed structure becomes more flexible. Especially, at high frequencies, the sliding boundary condition at the excitation point results in a reduction by a factor of 2 in the average level of the point mobility of the framed structure compared with the less constrained case. At very low frequency the difference is larger due to the effect of rotation of the frame on the effective mass.

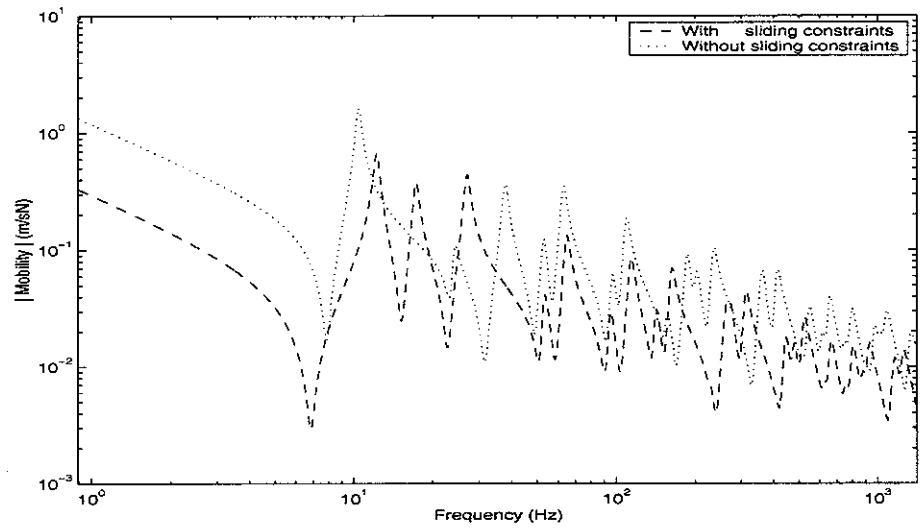

Figure B.3. Point mobility comparison to identify the effect of the rotational constraints on the beam frame structure using FE (excitation at $x = 0$ and $y = 0$).